WL-TR-93-4043

ELASTIC-PLASTIC FINITE-DIFFERENCE ANALYSIS OF UNIDIRECTIONAL COMPOSITES SUBJECTED TO THERMOMECHANICAL CYCLIC LOADING

Demirkan Coker and Noel E. Ashbaugh

University of Dayton Research Institute
300 College Park
Dayton, OH 45469-0001

December 1992
Final Report for 01/01/92-12/01/92

Approved for Public Release; Distribution is Unlimited

Materials Directorate
Wright Laboratory
Air Force Materiel Command
Wright Patterson AFB OH 45433-7734

NOTICE

When Government drawings, specifications, or other data are used for any purpose other than in connection with a definitely Government-related procurement, the United States Government incurs no responsibility or any obligation whatsoever. The fact that the government may have formulated or in any way supplied the said drawings, specifications, or other data, is not to be regarded by implication, or otherwise in any manner construed, as licensing the holder, or any other person or corporation; or as conveying any rights or permission to manufacture, use, or sell any patented invention that may in any way be related thereto.

This report is releasable to the National Technical Information Service (NTIS). At NTIS, it will be available to the general public, including foreign nations.

This technical report has been reviewed and is approved for publication.

Jay R Jira

JAY R. JIRA
Project Engineer
Materials Behavior Branch

Allan W Gunderson

ALLAN W. GUNDERSON, Chief
Materials Behavior Branch
Metals and Ceramics Division

Norman M Geyer

NORMAN M. GEYER
Acting Deputy Chief
Metals and Ceramics Division
Materials Directorate

If your address has changed, if you wish to be removed from our mailing list, or if the addressee is no longer employed by your organization please notify WL/MLLN , WPAFB, OH 45433-7817 to help us maintain a current mailing list.

Copies of this report should not be returned unless return is required by security considerations, contractual obligations, or notice on a specific document.

REPORT DOCUMENTATION PAGE

Form Approved
OMB No. 0704-0188

1. AGENCY USE ONLY (Leave blank)	2. REPORT DATE	3. REPORT TYPE AND DATES COVERED
	December 1992	Interim: January 1992-December 1992

4. TITLE AND SUBTITLE
Elastic-Plastic Finite-Difference Analysis of Unidirectional Composites Subjected to Thermomechanical Cyclic Loading

5. FUNDING NUMBERS
F33615-91-C-5606
PE-61102
PR-2302
TA-P1
WU-03

6. AUTHOR(S)
Demirkan Coker and Noel E. Ashbaugh

7. PERFORMING ORGANIZATION NAME(S) AND ADDRESS(ES)
University of Dayton Research Institute
300 College Park
Dayton, OH 45469-0001

8. PERFORMING ORGANIZATION REPORT NUMBER

9. SPONSORING/MONITORING AGENCY NAME(S) AND ADDRESS(ES)
Materials Directorate
Wright Laboratory
Air Force Materiel Command
Wright-Patterson Air Force Base, OH 45433-7734

10. SPONSORING/MONITORING AGENCY REPORT NUMBER
WL-TR-93-4043

11. SUPPLEMENTARY NOTES

12a. DISTRIBUTION/AVAILABILITY STATEMENT
Approved for public release; distribution is unlimited.

12b. DISTRIBUTION CODE

13. ABSTRACT *(Maximum 200 words)*

An analytical tool was developed to model a unidirectional composite subjected to thermomechanical cyclic loading and processing conditions. The finite difference method was incorporated into a PC compatible computer code, FIDEP (Finite-Difference Code for Elastic-Plastic Analysis of Composites). FIDEP provides an efficient numerical procedure for analyzing a variety of problems involving thermal and mechanical cycling. The procedure allows the modeling of the constituent materials as elastic-plastic with temperature dependent properties. The concentric cylinder approximation allows the computations to capture the three-dimensional aspects of the stress state in a real composite. Results for a thermal cool-down in an SCS-6/Ti-24Al-11Nb unidirectional composite compare well with those obtained using the finite element method. Several problems were solved for thermomechanical loading conditions and demonstrate the three-dimensional nature of the stress fields in the matrix material.

14. SUBJECT TERMS
Concentric cylinder model, elastic plastic, finite difference methods, metal matrix composite, thermomechanical fatigue, unidirectional composite.

15. NUMBER OF PAGES
90

16. PRICE CODE

17. SECURITY CLASSIFICATION OF REPORT	18. SECURITY CLASSIFICATION OF THIS PAGE	19. SECURITY CLASSIFICATION OF ABSTRACT	20. LIMITATION OF ABSTRACT
Unclassified	Unclassified	Unclassified	UL

TABLE OF CONTENTS

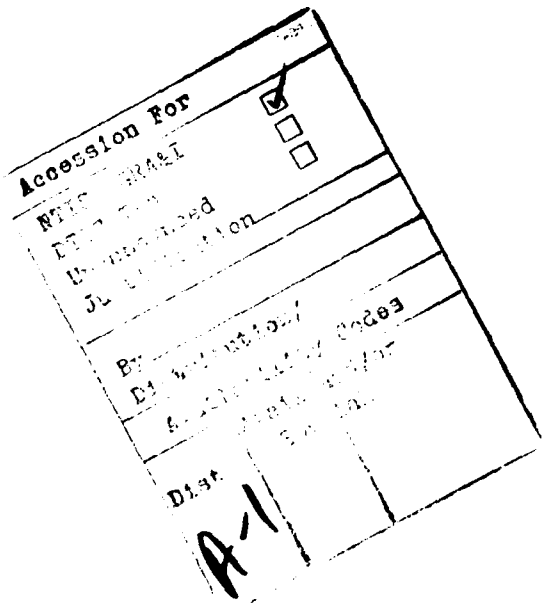

LIST OF FIGURES

LIST OF TABLES

FOREWORD

This report documents a computer program that was developed as part of an investigation of the mechanical behavior of metal matrix composites. The investigators were Demirkan Coker and Noel E. Ashbaugh of the Structural Integrity Division, University of Dayton Research Institute, Dayton OH. The research was conducted at the Materials Behavior Branch, Metals and Ceramics Division, Materials Directorate, Wright Laboratory (WL/MLLN) Wright-Patterson AFB OH, under Contract No. F33615-91-C-5606. The contract was administered under the direction of WL/MLLN by Mr. Jay R. Jira. Dr. Noel E. Ashbaugh was the Principal Investigator and Dr. Joseph P. Gallagher was the Program Manager.

CHAPTER 1
INTRODUCTION

Interest in metal matrix composites (MMC) for high-temperature aerospace applications has grown in recent years. Because of the high use temperatures envisioned, proposed applications of MMCs almost always involve both thermal and mechanical cyclic loading. Consequently, the accurate prediction of the thermomechanical fatigue (TMF) life of these components is a critical aspect of the design process. Because of the mismatch in coefficient of thermal expansion between fiber and matrix, internal thermal stresses are produced during cool-down from the processing temperature and subsequent thermal cycling. These stresses must be accounted for in the analysis in addition to those produced by mechanical loading. Prediction of the mechanical behavior and life of a composite material, therefore, requires a knowledge of the individual components of stress or strain in the fiber and/or matrix as well as the overall applied stresses.

In this investigation, an axisymmetric concentric cylinder geometry was used to model the unidirectional composite in which the fiber and matrix were represented by the core cylinder and outer cylinder, respectively. The concentric cylinder geometry allowed for a relatively simplified analysis and was adequate for predicting the complex three-dimensional stress distributions in the fiber and the matrix. The analysis allowed for axial and radial loading and more than two constituents with bilinear elastic-plastic properties. The analysis also accounted for thermomechanical loading and temperature dependent material properties. These aspects were incorporated into a FORTRAN program, FIDEP (**Fi**nite **D**ifference **C**ode for **E**lastic-**P**lastic Analysis).

This report summarizes the derivation and application of the concentric cylinder model to predict the micromechanical stresses in an SCS-6/Ti-24Al-11Nb metal matrix composite. The next chapter summarizes some of the past work done on micromechanical modeling of composites. Chapter 3 describes the theory for the concentric cylinder model and summarizes plasticity theory. In Chapter 4 the implementation of the theory to the computer program, FIDEP, is described and the procedures for using this program are explained in Chapter 5. Finally some example runs are conducted with this program and the results are presented .

CHAPTER 2
BACKGROUND

Various approaches have been adopted in the past to calculate the micromechanical stresses in the fiber and the matrix due to both thermal and mechanical loading. The most widespread approach involves use of the finite element method to model a representative volume element (RVE) and compute the stress distributions around the fiber. Common RVE geometries that have been used include either a square or a cylindrical fiber in a square matrix and a cylindrical fiber in a cylindrical matrix. Different constitutive behaviors include elastic-plastic behavior [1-3], time-dependent behavior using a classical creep law [4] and unified viscoplastic theories such as the Bodner-Partom model [5], and Bodner-Partom with backstress [6]. However, finite element codes are usually run on mainframe computers, are time consuming, allow for solution of only one problem at a time, and require familiarity with finite element analysis and the code. To conduct a parametric study and to support the design of a large number of experiments on different composite systems, a more practical approach is desirable.

One simple approach to micromechanical modeling of composites has been to use average stresses in the constituents. This method has the advantage of being easy to implement into a code and of easily being extended to analyze laminates. Approaches using this method include analysis of square fiber in a square matrix and the vanishing fiber diameter (VFD) model developed by Dvorak and Bahei-El-Din [7]. In the VFD model, the presence of the fibers is assumed not to influence the transverse stresses. The transverse properties of a lamina are easily computed using this assumption while the longitudinal properties are calculated from the rule of mixtures. This analysis can be carried out for an elastic fiber surrounded by a matrix material having a variety of constitutive relations to calculate ply properties which, in turn, can be incorporated into lamination theory to analyze a composite. Such a procedure has been implemented into computer codes such as AGLPLY [8] which uses thermoplastic matrix behavior and VISCOPLY [9] which incorporates the Eisenberg creep model to predict average stresses in the constituents and in a symmetric composite laminate subjected to thermomechanical loading. Aboudi [10] modeled a square fiber in a square matrix subcell using first order displacement expansions. The unified theory of Bodner and Partom was used to compute inelastic strains. Hopkins and Chamis [11] and Sun [12] conducted strength-of-materials type analyses for a square fiber in a square matrix cell to obtain expressions for the constituent microstresses. Chamis

and Hopkins [13] modified these expressions based on experimental data for uniaxial lamina and three-dimensional computer simulations of composite behavior. The results were incorporated into a computer program, METCAN [14], which treats material nonlinearity at the constituent level where material behavior is modeled using a time-temperature-stress dependence of constituent properties.

The main drawback to all of these simplified material models is the assumption of average uniform stress in the representative volume element. This approach fails to take into account the triaxial stresses that arise due to the mismatch of the Poisson's ratio and the coefficient of thermal expansion of the constituents. A detailed review of these codes and comparisons of the stresses using these methods and using finite element analysis is given by Bigelow et al. [15].

For a more accurate analytical treatment of the triaxial stresses, the concentric cylinder model has been used in the literature due to its simple geometry. Thermoelastic treatment of the axisymmetric concentric cylinder model with multiple rings are given in references [16, 17]. An elastic analysis of a multidirectional coated continuous fiber composite by means of a three-phase concentric cylinder model is given in reference [18]. Ebert et al. [19] and Hecker et al. [20] were the first to introduce elastic-plastic behavior for the constituents in which they modeled two concentric cylinders and verified the model with experiments. Gdoutos et al. used this model to compute thermal expansion coefficients [21] and stress-strain curves and obtained good agreement with experimental results [22]. However, this approach postulated new stress-strain relations in which the strain increments were functions of the stress increment, in contrast to the Prandtl-Reuss relations that relate the strain increments to the current state of stress. This method is a deformation type of theory and could not be applied to nonproportional loadings and ideally plastic material. More recently Lee and Allen [23] obtained an analytical solution for elastic-perfectly plastic fiber and matrix obeying Tresca's yield criterion.

In this investigation an analytical tool was developed to compute the three-dimensional stress state in a composite using the concentric cylinder model. The analysis accommodates multiple materials having elastic-plastic behavior with strain hardening. The Prandtl-Reuss flow rule with the von Mises yield criterion was used. In addition, temperature-dependent material properties were taken into account. The analysis was implemented into the computer code FIDEP (Finite Difference Code for Elastic-Plastic Analysis of Composites) which accounts for thermomechanical cyclic loading.

CHAPTER 3
THEORY

The derivations of the elastic-plastic concentric cylinder equations are described in this section. The solution technique for the numerical integration of the Prandtl-Reuss equations are also summarized.

3.1 Concentric Cylinder Model

A representative volume element of the composite is modeled as concentric cylinders with the core cylinder representing the fiber and the outer ring representing the matrix (Fig. 3.1). The fiber and matrix radii are denoted as a and b, respectively. The direction of the z-axis is along the fibers and the cylinders are infinitely long in the axial direction. Cylindrical coordinates are used in the equations.

The following assumptions are made in the analysis. The temperature distribution is uniform and is quasi-static. A perfect bond exists between the constituents of the composite so that there is no slippage or separation of the constituents. The concentric cylinders are in generalized plane strain and are subjected to axisymmetric loadings and displacements so that the shear stresses are zero. The constituent properties are isotropic. The fiber is linearly elastic. The matrix follows a von Mises yield surface and is incompressible in the plastic region, i.e., hydrostatic stresses do not cause plastic deformation. The plastic deformation of the matrix is governed by the Prandtl-Reuss flow rule.

The following boundary conditions are imposed:

1) radial stress is P_r at r=b,

2) finite stresses at r=0, and

3) continuous radial displacements and radial stresses at the interface.

3.2 Governing Equations

Equilibrium and compatibility equations in cylindrical coordinates for an axisymmetric generalized-plane strain case simplify to [24]:

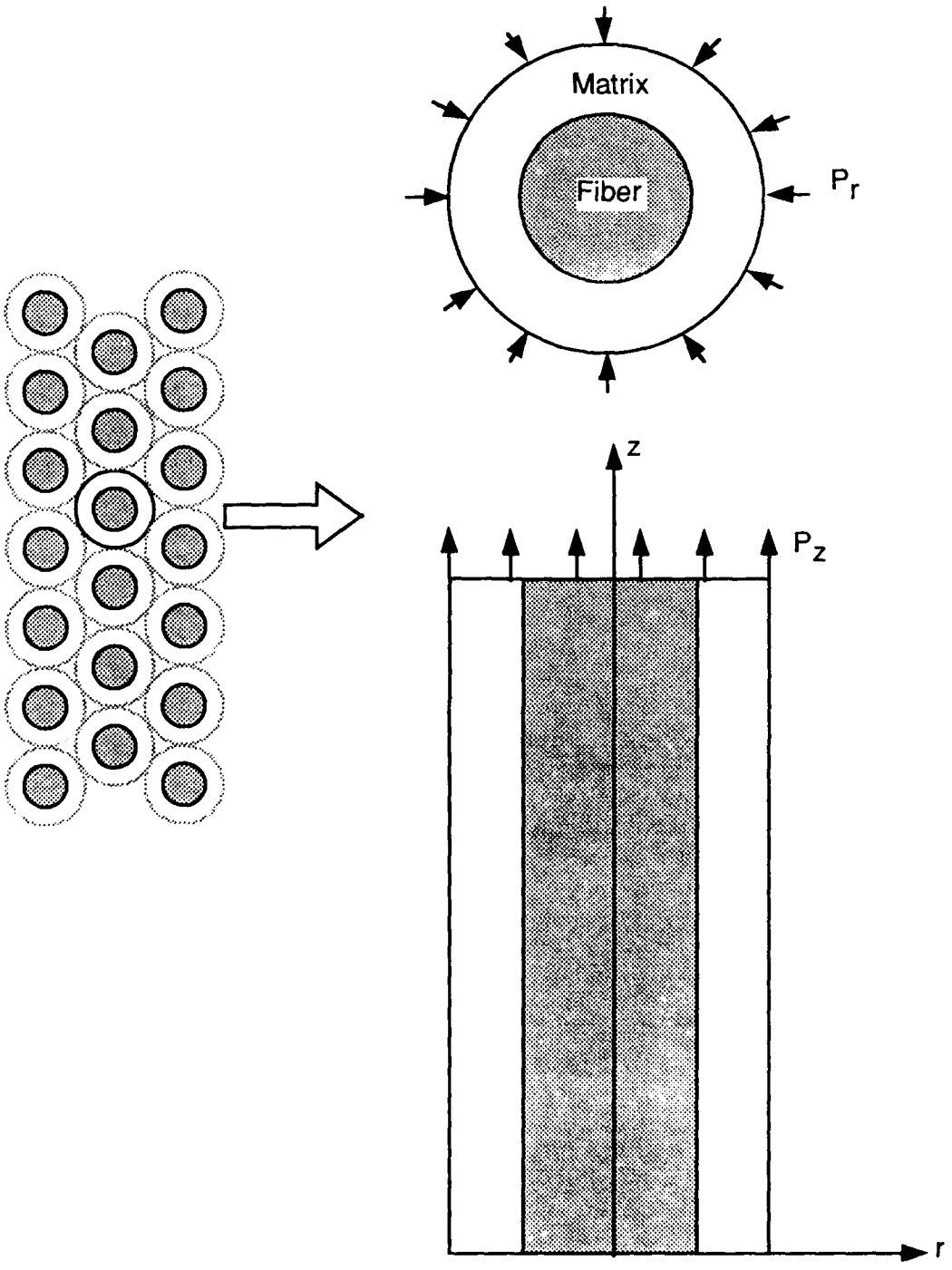

Fig. 3.1 Concentric Cylinder Idealization of a Unidirectional Composite and the Concentric Cylinder Model.

$$\frac{d\sigma_r}{dr}+\frac{\sigma_r-\sigma_\theta}{r}=0, \tag{1}$$

$$\frac{d\varepsilon_\theta}{dr}-\frac{\varepsilon_r-\varepsilon_\theta}{r}=0, \tag{2}$$

and the stress-strain equations are [25]:

$$\begin{aligned}
\varepsilon_r &= \frac{1}{E}(\sigma_r-\nu(\sigma_\theta+\sigma_z))+\alpha T+\varepsilon_r^p+d\varepsilon_r^p,\\
\varepsilon_\theta &= \frac{1}{E}(\sigma_\theta-\nu(\sigma_r+\sigma_z))+\alpha T+\varepsilon_\theta^p+d\varepsilon_\theta^p,\\
\varepsilon_z &= \frac{1}{E}(\sigma_z-\nu(\sigma_r+\sigma_\theta))+\alpha T+\varepsilon_z^p+d\varepsilon_z^p
\end{aligned} \tag{3}$$

where ε_r^p, ε_θ^p and ε_z^p are the total accumulated plastic strains up to, but not including the current increment of loading, $d\varepsilon_r^p$, $d\varepsilon_\theta^p$ and $d\varepsilon_z^p$ are the plastic strain increments due to the current increment of loading, ε_r, ε_θ and ε_z are the total strains, σ_r, σ_θ and σ_z are the stresses, α is the secant coefficient of thermal expansion (CTE), ν is the Poisson's ratio, E is the Young's modulus and T is the change in temperature from a reference state in which the stresses and the strains are assumed to be zero.

Substitution of Eqn. 3 into Eqn. 2 to eliminate total radial and hoop strains yields:

$$\begin{aligned}
&\frac{d}{dr}\left(\frac{\sigma_\theta}{E}-\frac{\nu}{E}\left(\sigma_r+\nu(\sigma_r+\sigma_\theta)-\alpha ET+E(\varepsilon_x-\varepsilon_z^p-d\varepsilon_z^p)\right)+\alpha T+\varepsilon_\theta^p+d\varepsilon_\theta^p\right)\\
&+\frac{(1+\nu)}{Er}(\sigma_\theta-\sigma_r)+\frac{\varepsilon_\theta^p+d\varepsilon_\theta^p-\varepsilon_r^p-d\varepsilon_r^p}{r}=0
\end{aligned} \tag{4}$$

This equation together with the equilibrium equation results in two ordinary differential equations in the two unknowns, σ_r and σ_θ. The axial strain, ε_z, is a constant value across the cross section because of the imposed generalized plane strain condition.

3.3 Computation of the Axial Strain

To compute the axial strain, the stress-strain equation in the axial direction (Eqn. 3) is multiplied by E r and integrated over the cross section:

$$\varepsilon_z \int_0^b E r dr = \int_0^b \sigma_z r dr - \int_0^b \nu(\sigma_r + \sigma_\theta) r dr + \int_0^b \alpha E T r dr + \int_0^b E(\varepsilon_z^p + d\varepsilon_z^p) r dr. \qquad (5)$$

For k concentric cylinders, let a_i be the outer radius of the ith ring and $a_0 = 0$, then the integral on the left hand side reduces to:

$$\varepsilon_z \int_0^b E r dr = \varepsilon_z \sum_{i=1}^{k} \frac{E_i}{2}(a_i^2 - a_{i-1}^2). \qquad (6)$$

The first integral on the right hand side is evaluated using the global equilibrium equation in the axial direction; i. e. internal forces are equal to the external applied forces:

$$\int_0^b \sigma_z (2\pi r) dr = P_z(\pi r^2), \qquad (7)$$

where P_Z is the applied axial stress.

Rearranging the terms, the equilibrium equation (Eqn. 1) can also be written as [26]:

$$(\sigma_r + \sigma_\theta) r = \frac{d}{dr}(r^2 \sigma_r). \qquad (8)$$

Using Eqn. 8, the second integral on the right hand side of Eqn. 5 becomes:

$$\int_0^b \nu \frac{d}{dr}(r^2 \sigma_r) dr = \sum_{i=1}^{k} \nu_i (a_i^2 \sigma_r(a_i) - a_{i-1}^2 \sigma_r(a_{i-1})), \qquad (9)$$

Expanding and recollecting terms in Eqn. 9:

$$\int_0^b \nu \frac{d}{dr}(r^2 \sigma_r) dr = \sum_{i=1}^{k-1} (\nu_i - \nu_{i-1}) a_i^2 \sigma_r(a_i) + \nu_k b^2 \sigma_r(b), \qquad (10)$$

where $\sigma_r(b)$ is the applied radial stress at r=b.

The remaining terms are similarly evaluated assuming constant material properties and temperature distribution in each cylinder. The axial strain for k concentric cylinders then becomes:

$$\varepsilon_z = \frac{1}{E_c}\left\{P_z - 2\sum_{i=1}^{k-1} V_i \sigma_r(a_i)(\nu_i - \nu_{i+1}) - 2\nu_k \sigma_r(b) + \alpha_c E_c T + \frac{2}{b^2}\sum_{i=1}^{k} E_i \int_0^b (\varepsilon_z^p + d\varepsilon_z^p) r dr\right\}, \quad (11)$$

where, V_i is the volume fraction of the ith cylinder, E_c is the axial composite modulus and α_c is the axial coefficient of thermal expansion of the composite defined by:

$$V_i = \frac{a_i^2 - a_{i-1}^2}{b^2},$$

$$E_c = \sum_{i=1}^{k} E_i V_i,$$

and

$$\alpha_c = \frac{\sum_{i=1}^{k} \alpha_i E_i V_i}{E_c}.$$

In the case of two concentric cylinders representing an elastic fiber and an elastic-plastic matrix, k = 2 and $\varepsilon_z^p = 0$ in the fiber, so that the expression for the axial strain simplifies to:

$$\varepsilon_z = \frac{1}{E_c}\left\{P_z - 2V_f(\nu_f - \nu_m)\sigma_r(a) - 2\nu_m P_r + \alpha_c E_c T + \frac{2E_m}{b^2}\int_a^b (\varepsilon_z^p + d\varepsilon_z^p) r dr\right\}, \quad (12)$$

where

$$\alpha_c = \frac{1}{E_c}(\alpha_f E_f V_f + \alpha_m E_m V_m),$$

$$E_c = E_f V_f + E_m V_m,$$

and V_f and V_m are the fiber and matrix volume fractions, respectively, and P_r is the applied radial stress at r=b. In Eqs. 11 and 12, the axial strain is written in terms of the radial stresses at the interfaces. The total plastic strains are known from the previous loading steps and the new plastic strain increments are related to the stresses through the Prandtl-Reuss flow rule.

Note that if the Poisson's ratio for the cylinders is the same and the applied radial stress is zero, the second and third terms vanish leaving the total axial strain as the sum of the composite elastic strain (ε_z^{cc}), composite thermal strain (ε_z^{thc}) and composite plastic strain (ε_z^{pc}), i. e.:

$$\varepsilon_z^c = \varepsilon_z^{ec} + \varepsilon_z^{thc} + \varepsilon_z^{pc} = \frac{P_z}{E_c} + \alpha_c T + \frac{2}{b^2}\frac{E_m}{E_c}\int_a^b (\varepsilon_z^p + d\varepsilon_z^p) r dr .$$

If the plastic strain is constant throughout the matrix, then we have for the total strain:

$$\varepsilon_z^c = \frac{P_z}{E_c} + \alpha_c T + \frac{E_m V_m}{E_c}\varepsilon_z^{pm} ,$$

where ε_z^{pm} is the average matrix plastic strain.

3.4 Finite Difference Formulation

The method of finite differences is used to solve the two ordinary differential equations [25]. The disk radius is divided into N intervals as shown in Fig. 3.2. There are thus N+1 stations, the first station being at the center of the disk and the last station at the outer radius. Eqs. 1 and 4 are written in finite difference form at midpoints of these intervals as follows:

$$r_{i-\frac{1}{2}} = \frac{r_i - r_{i-1}}{2} , \quad \frac{d}{dr}\sigma_{r,i-\frac{1}{2}} = \frac{\sigma_{r,i} - \sigma_{r,i-1}}{r_i - r_{i-1}} ,$$

$$\sigma_{r,i-\frac{1}{2}} = \frac{\sigma_{r,i} - \sigma_{r,i-1}}{2} , \quad \frac{d}{dr}\left(\frac{\sigma_\theta}{E}\right)_{i-\frac{1}{2}} = \frac{\sigma_{\theta,i}/E_i - \sigma_{\theta,i-1}/E_{i-1}}{r_i - r_{i-1}} ,$$

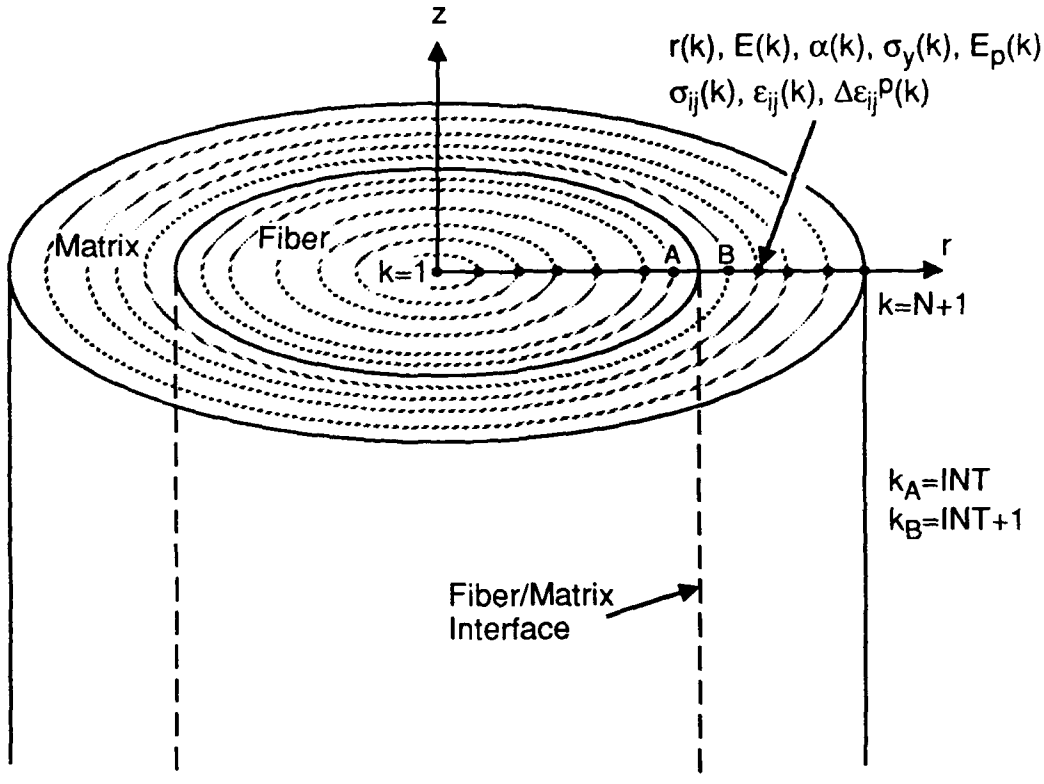

Fig. 3.2 Discretization of the Concentric Cylinder Model.

$$(1+\nu)\frac{\sigma_\theta}{Er}\bigg|_{i-\frac{1}{2}} = \frac{1}{2}\frac{(1+\nu_i)\sigma_{\theta,i}/E_i - (1+\nu_{i-1})\sigma_{\theta,i-1}/E_{i-1}}{r_i - r_{i-1}/2}\ , \text{etc.}$$

In this manner Eqs. 1 and 4 can be written at the midpoints of n stations resulting in 2n equations;

$$\left.\begin{aligned} &\frac{1}{c_i}\sigma_{r,i-1} - \sigma_{r,i} + a_i\sigma_{\theta,i-1} + a_i\sigma_{\theta,i} = 0 \\ &G_i\sigma_{r,i-1} + D_i\sigma_{r,i} + H_i\sigma_{\theta,i-1} - F_i\sigma_{\theta,i} = Q_i - P_i \end{aligned}\right\} \quad i = 2,\ldots,n+1, \qquad (13)$$

where

$$a_i = (r_i - r_{i-1})/2r_i\ ,\quad b_i = E_i/E_{i-1}\ ,\quad c_i = r_i/r_{i-1}\ ,$$

and

$$D_i = (1+\nu_i)(\nu_i + a_i)\ ,$$

$$F_i = (1+\nu_i)(1-\nu_i + a_i)\ ,$$

$$G_i = b_i(1+\nu_{i-1})(\nu_{i-1} - a_i c_i)\ ,$$

$$H_i = b_i(1+\nu_{i-1})(1-\nu_{i-1} - a_i c_i)\ ,$$

$$Q_i = E_i T(\alpha_i(1+\nu_i) - \alpha_{i-1}(1+\nu_{i-1}))\ ,$$

$$P_i = E_i(P_i^* + \varepsilon_z(\nu_i - \nu_{i-1}))\ ,$$

$$\begin{aligned} P_i^* = {} & \nu_i(\varepsilon_{r,i}^{p+} + \varepsilon_{\theta,i}^{p+}) - \nu_{i-1}(\varepsilon_{r,i-1}^{p+} + \varepsilon_{\theta,i-1}^{p+}) \\ & + a_i\left[\varepsilon_{r,i}^{p+} + c_i\varepsilon_{r,i-1}^{p+} - \varepsilon_{\theta,i}^{p+}(1/a_i + 1) + \varepsilon_{\theta,i-1}^{p+}(1/a_i - c_i)\right]\ , \end{aligned}$$

where the plastic strains, $\varepsilon_{r,i}^{p+}$, etc., are the updated plastic strains, i. e. $\varepsilon_{r,i}^{p+} = \varepsilon_{r,i}^{p} + d\varepsilon_{r,i}^{p}$, etc. The coefficients at the left hand side are functions of material properties at the ith station. Only the P* term on the right hand side involves plastic strains. The unknowns are $\sigma_{r,i}$ and $\sigma_{\theta,i}$, i = 1,...,n+1. Using the boundary conditions, $\sigma_{r,n+1} = P_r$ and $\sigma_{\theta,1} = \sigma_{r,1}$, the

unknowns reduce to 2n; $\sigma_{r,i}$, i=1,...,n, and $\sigma_{\theta,i}$, i=2,...,n+1. The axial stress distribution, $\sigma_{z,i}$, i=1,...,n+1, is given by Eqn. 3.

Moving the radial stress terms in Eqn. 11 to the left hand side of Eqn. 13 and letting the radial stress at the jth interface correspond to the radial stress at node i=I_j, i. e., $\sigma_r(a_j) = \sigma_{r,I_j}$, the second expression in Eqs. 13 becomes:

$$\begin{aligned} -G_i\sigma_{r,i-1} + D_i\sigma_{r,i} + H_i\sigma_{\theta,i-1} - F_i\sigma_{\theta,i} - 2(\nu_i - \nu_{i-1})\frac{E_i}{E_c}\sum_{j=1}^{k-1} V_j\sigma_{r,I_j}(\nu_{I_j} - \nu_{I_j+1}) \\ = Q_i - E_iP_i^* - E_i(\nu_i - \nu_{i-1})\varepsilon_z^* \end{aligned} \quad (14)$$

where

$$\varepsilon_z^* = \frac{1}{E_c}(P_z - 2\nu_k P_r + \alpha_c E_c T + 2/b^2 \sum_{j=1}^{k} E_j \int_0^b \varepsilon_z^{p+} r dr). \quad (15)$$

In the case of two concentric cylinders, k=2 and j=1. Let INT be defined as the index of the highest-numbered node in the fiber and INT+1 be the index of the lowest-numbered node in the matrix. The fiber-matrix interface lies between these two nodes. Then, for all equations in which i ≠ INT+1, i. e., equations for nodes not adjacent to the interface, n_i-n_{i-1} is zero and the axial strain vanishes from these equations. For the INT+1st equation, Eqn. 14 reduces to:

$$\begin{aligned} &(2V_fE_m/E_c(\nu_f - \nu_m)^2 - G_{INT+1})\sigma_{r,INT} \\ &+D_{INT+1}\sigma_{r,INT+1} + H_{INT+1}\sigma_{\theta,INT} + F_{INT+1}\sigma_{\theta,INT+1}. \\ &= Q_{INT+1} - E_mP_{INT+1}^* - E_m(\nu_m - \nu_f)\varepsilon_z^* \end{aligned} \quad (16)$$

One final step before Eqs. 13 are written in matrix form is to eliminate singular terms for i=2. Note that $\sigma_{r,1} = \sigma_{\theta,1}$. Thus $\sigma_{r,1}$ and $\sigma_{\theta,1}$ terms can be combined in Eqn. 13 to obtain:

$$\begin{aligned} (1/c_2 + a_2)\sigma_{r,1} - \sigma_{r,2} + a_2\sigma_{\theta,2} = 0 \\ (H_2 - G_2)\sigma_{r,1} + D_2\sigma_{r,2} - F_2\sigma_{\theta,2} = Q_2 - P_2 \end{aligned}$$

In the first equation $1/c_2 = r_1/r_2 = 0$. In the second equation, the term H_2-G_2 is expanded and simplified. The final equations for i=2 become:

$$a_2\sigma_{r,1} - \sigma_{r,2} + a_2\sigma_{\theta,2} = 0$$
$$(1+\nu_1)(1-2\nu_1)b_2\sigma_{r,1} + D_2\sigma_{r,2} - F_2\sigma_{\theta,2} = Q_2 - P_2$$

Hence Eqn. 13 is written in matrix form as:

$$\underline{A}\,\underline{x} = \underline{B}\,, \tag{17}$$

where $\underline{A}$ is a 2n by 2n matrix of constant coefficients, $\underline{x}$ is the radial and hoop stress vector of length 2n and $\underline{B}$ is a vector of length 2n, as shown in Fig. 3.3. In matrices $\underline{A}$ and $\underline{B}$ all the constants are known except the plastic strain increments which are presumed or computed from the Prandtl-Reuss relations.

3.5 Plasticity Theory

The plastic strains increments are computed using Prandtl-Reuss relations [25]. In this section two forms of the Prandtl-Reuss equations are summarized; equations relating plastic strain increments to stresses and equations relating plastic strain increments to modified total strains.

3.5.1 Prandtl-Reuss Relations

Prandtl and Reuss assumed that the plastic strain increment is proportional to the instantaneous stress deviation, i. e.:

$$d\varepsilon_{ij}^{p} = \lambda S_{ij} \tag{18}$$

where S_{ij} is the deviatoric stress tensor and λ is a nonnegative constant which may vary throughout the loading history. These equations imply that the plastic strain increments depend on the current stress state and not on the stress increment required to reach this state. To determine λ, both sides are squared and multiplied by 2/3 to obtain:

$$\frac{2}{3}d\varepsilon_{ij}^{p}d\varepsilon_{ij}^{p} = \frac{2}{3}\lambda^2 S_{ij}S_{ij} \tag{19}$$

Define effective plastic strain increment and effective stress, respectively, as:

$\underline{\underline{A}}\underline{x} = \underline{b}$, $\underline{\underline{A}}$ = Matrix of material properties, $\underline{x} = \begin{bmatrix} \underline{\sigma}_r \\ \underline{\sigma}_\theta \end{bmatrix}$, $\underline{b} = \begin{bmatrix} \underline{0} \\ \underline{Q} - \underline{P}(\underline{\Delta\varepsilon}_{ij}) \end{bmatrix}$

a_2	-1	0	0	...	0	0	a_2	0	0	...	0	0	0	$\sigma_{r,1}$		0
0	$1/c_3$	-1	0	...	0	0	a_3	a_3	0	...	0	0	0	$\sigma_{r,2}$		0
0	0	$1/c_4$	-1	...	0	0	0	a_4	a_4	...	0	0	0	⋮		⋮
0	0	0	0	...	$1/c_N$	-1	0	0	0	...	a_N	a_N	0	$\sigma_{r,N-1}$		0
0	0	0	0	...	0	$1/c_{N+1}$	0	0	0	...	0	a_{N+1}	a_{N+1}	$\sigma_{r,N}$	=	$\sigma_{r,b}$
H_2-G_2	D_2	0	0	...	0	0	- F_2	0	0	...	0	0	0	$\sigma_{\theta,2}$		Q_2-P_2
0	- G_3	D_3	0	...	0	0	H_3	- F_3	0	...	0	0	0	$\sigma_{\theta,3}$		Q_3-P_3
														⋮		⋮
		...	G*	...												
0	0	0	0	...	- G_N	D_N	0	0	0	...	H_N	- F_N	0	$\sigma_{\theta,N}$		Q_N-P_N
0	0	0	0	...	0	-G_{N+1}	0	0	0	...	0	H_{N+1}	-F_{N+1}	$\sigma_{\theta,N+1}$		Q_{N+1} - $P_{N+1}\sigma_{r,b}$

$$G^* = A(N + INT, INT) = 2V_f(v_f - v_m)^2 E_m / E_c - G_{INT+1}$$

Figure 3.3 The Linear System of Equations Resulting from the Finite Differences Formulation of the Governing Equations for the Concentric Cylinder Model.

$$de^p = \sqrt{\frac{2}{3} d\varepsilon_{ij}^p d\varepsilon_{ij}^p} \quad \text{and} \quad \sigma_{eff} = \sqrt{\frac{2}{3} S_{ij} S_{ij}} . \tag{20}$$

Using these definitions λ is determined from Eqn. 20 as:

$$\lambda = \frac{3}{2} \frac{de^p}{\sigma_{eff}} \tag{21}$$

and the Prandtl-Reuss relations become:

$$d\varepsilon_{ij}^p = \frac{3}{2} \frac{de^p}{\sigma_{eff}} S_{ij}. \tag{22}$$

These equations are used together with the von Mises yield criterion. Yielding begins when the effective stress reaches the yield stress determined from a uniaxial tensile test.

3.5.2 Plastic Strain-Total Strain Plasticity Relations

The above form of the Prandtl-Reuss relations relate the plastic strain increments to the stresses. Another method to computing the plastic strain increments is to use equations that relate the plastic strain increments to the modified total strains. These equations will be more stable with respect to the loading increment size and converge faster for most loading cases. In this approach the plastic strain increments are computed using modified Prandtl-Reuss relations derived by Mendelson [25].

Assume a loading path to a given state of stress and total plastic strains ε_{ij}^p and let the next load step be applied producing additional plastic strains $\Delta\varepsilon_{ij}^p$. The total strains can be written as:

$$\varepsilon_{ij} = \varepsilon_{ij}^e + \varepsilon_{ij}^{th} + \varepsilon_{ij}^p + \Delta\varepsilon_{ij}^p, \tag{23}$$

where ε_{ij}^e is the elastic component of the total strain, ε_{ij}^{th} is the thermal strain, ε_{ij}^p is the accumulated plastic strain up to (but not including) the current increment of load, and $\Delta\varepsilon_{ij}^p$ is the increment of plastic strain due to the increment of load. The previous plastic strains ε_{ij}^p are presumed to be known, and $\Delta\varepsilon_{ij}^p$ is to be calculated.

The modified total strains are defined as:

$$\varepsilon'_{ij} = \varepsilon_{ij} - \varepsilon^{p}_{ij} = \varepsilon^{e}_{ij} + \varepsilon^{th}_{ij} + \Delta\varepsilon^{p}_{ij}. \tag{24}$$

The deviatoric strains are obtained by subtracting the mean strain from the diagonal component of both sides:

$$e'_{ij} = e^{e}_{ij} + \Delta e^{p}_{ij}. \tag{25}$$

where ε_{ij}^{e} is the elastic strain deviator tensor and ε_{ij}' is the modified strain deviator tensor. From Hooke's Law and Prandtl-Reuss Eqn. 18:

$$e^{e}_{ij} = \frac{S_{ij}}{2G} = \frac{\Delta e^{p}_{ij}}{2G\lambda}, \tag{26}$$

where G is the shear modulus. Using this expression and Eqn. 18, Eqn. 25 becomes:

$$e'_{ij} = (1 + \frac{1}{2G\lambda}) de^{p}_{ij}.$$

Multiplying both sides of the equation by two thirds itself:

$$\frac{2}{3} e'_{ij} e'_{ij} = \frac{2}{3} (1 + \frac{1}{2G\lambda})^{2} de^{p}_{ij} de^{p}_{ij}.$$

Define effective modified total strain in a similar fashion to the effective incremental plastic strain rate to obtain:

$$e'_{eff} = (1 + \frac{1}{2G\lambda}) de^{p}. \tag{27}$$

The modified Prandtl-Reuss relations then become:

$$de^{p}_{ij} = \frac{de^{p}}{e'_{eff}} e'_{ij}, \tag{28}$$

where ε_{ij}' are the modified total deviatoric strains, ε'_{eff} is the equivalent or effective modified total strain defined by:

$$e'_{eff} = \sqrt{\frac{2}{3} e'_{ij} e'_{ij}}, \tag{29}$$

and $d\varepsilon_p$ is the equivalent or effective plastic strain increment defined by Eqn. 20. The modified Prandtl-Reuss equations in expanded form are:

$$d\varepsilon_x^p = \frac{d\varepsilon_{eff}^p}{3\varepsilon'_{eff}}(2\varepsilon'_x - \varepsilon'_y - \varepsilon'_z),$$

$$d\varepsilon_y^p = \frac{d\varepsilon_{eff}^p}{3\varepsilon'_{eff}}(2\varepsilon'_y - \varepsilon'_x - \varepsilon'_z),$$

$$d\varepsilon_z^p = \frac{d\varepsilon_{eff}^p}{3\varepsilon'_{eff}}(2\varepsilon'_z - \varepsilon'_x - \varepsilon'_y) = -(d\varepsilon_x^p + d\varepsilon_y^p)$$

$$d\varepsilon_{xy}^p = \frac{d\varepsilon_{eff}^p}{3\varepsilon'_{eff}}\varepsilon'_{xy}, \quad d\varepsilon_{yz}^p = \frac{d\varepsilon_{eff}^p}{3\varepsilon'_{eff}}\varepsilon'_{yz}, \quad d\varepsilon_{xz}^p = \frac{d\varepsilon_{eff}^p}{3\varepsilon'_{eff}}\varepsilon'_{xz}.$$

Equation 28 is equivalent to the Prandtl-Reuss Eqn. 18, but relate the incremental plastic strains to modified total strains instead of the stresses.

The relationship between the effective incremental plastic strain and effective modified total strain is obtained by substituting λ from Eqn. 21 in Eqn. 27:

$$\varepsilon'_{eff} = d\varepsilon_{eff}^p + \frac{1}{3G}\sigma_{eff}. \tag{30}$$

Let the effective stress from the previous loading step be $\sigma_{eff,i-1}$. By expanding the effective stress in a Taylor series about $\sigma_{eff,i-1}$:

$$\sigma_{eff} = \sigma_{eff,i-1} + \left(\frac{d\sigma_{eff}}{d\varepsilon_{eff}^p}\right)_{i-1} d\varepsilon_{eff}^p,$$

the effective stress is eliminated from Eqn. 30 to obtain:

$$d\varepsilon^{p}_{eff} = \frac{\varepsilon'_{eff} - \frac{1}{3G}\sigma_{eff,i-1}}{1+\frac{1}{3G}\left(d\sigma_{eff}/d\varepsilon^{p}_{eff}\right)_{i-1}}. \qquad (31)$$

The effective modified total strain has no physical significance and is purely a mathematical quantity even in the uniaxial case. In Eqn. 31 a small error in effective modified total strain or the effective stress will produce the same order-of-magnitude error in the effective plastic strain increment since the denominator is approximately unity. Equations 28, 29 and 31 are used simultaneously to determine plastic strain increments at each loading step.

3.6 Solution Technique

Solution of the elastic-plastic concentric cylinder problem requires the solution of 5 equations; the equilibrium and compatibility Eqs. 1 and 6, and the three Prandtl-Reuss relations (Eqn. 22 or 28). After elimination of the strains using the constitutive relations there are 6 unknowns left; σ_r, σ_θ, σz, $d\varepsilon_{rp}$, $d\varepsilon_{\theta p}$, $d\varepsilon_{zp}$. The axial stress is eliminated using Eqn. 11 reducing the number of unknowns to 5. The ordinary differential equations (Eqs. 1 and 6) are solved using the method of central finite differences to obtain a linear system of equations (Eqn. 13). These simultaneous equations are used in an iterative plasticity algorithm to solve for the stresses.

There are two iterative algorithms that were considered for this investigation both of which use forward-Euler integration scheme. The first algorithm uses the Prandtl-Reuss relations (Fig. 3.4). For an increment of load, a distribution is assumed for the plastic strain increments. The finite difference equations are then solved for a first elastic approximation to the stresses and strains. At the same time, the effective plastic strain increment is calculated (Eqn. 20). From the stress-strain curve the corresponding effective stress is computed. Finally, a new estimate computed for the plastic strain increments and these steps are repeated until convergence is obtained. This algorithm is not a very stable algorithm and may not converge for large load increments.

The second iterative method uses the modified version of the Prandtl-Reuss Eqn. 28 or the plastic strain-total strain relations developed by Mendelson [25]. This method is also called the elastic-predictor radial corrector method. In this algorithm (Fig. 3.5), total strains are obtained from the stresses from Eqn. 13 with assumed or previously calculated plastic

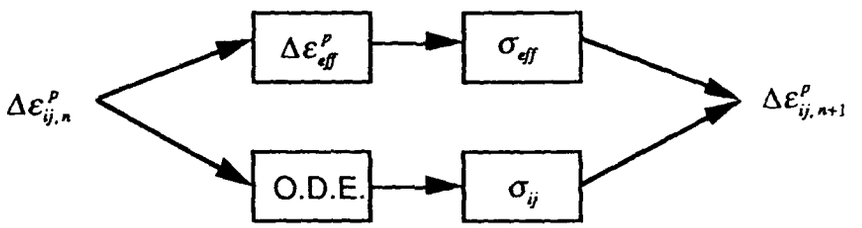

Figure 3.4 Schematic of the Iterative Technique for Computing Plastic Strains Using the Prandtl-Reuss Relations.

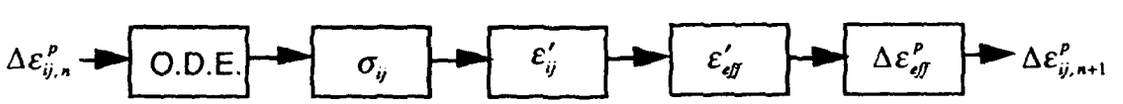

Figure 3.5 Schematic of the Iterative Technique for Computing Plastic Strains Using the Modified Prandtl-Reuss Relations.

strain increment estimates. Modified total strains and effective total strain are obtained from Eqs. 38 and stress-strain curve using Eqn. 43. The new plastic strain increments are then determined from Eqn. 40. This process is repeated until convergence of the plastic strains is obtained. This method converges for even large loading increments and converges very rapidly.

Both of these algorithms were implemented into the program FIDEP, Finite-Difference Code for Elastic-Plastic Analysis of Composites. However, since the first algorithm did not offer any advantage and was unstable except for very small time steps, the method using the modified plastic-strain total-strain relations was used.

CHAPTER 4
IMPLEMENTATION IN FIDEP

4.1 Algorithm

The algorithm and the pseudo-code for computing the stresses and plastic strain increments using the modified strain theory as implemented into the FORTRAN code FIDEP are shown in Figures 4.1 and 4.2. The procedure for calculating the stresses and strains is as follows:

1. A stress increment and a temperature increment are applied.
2. The finite difference equations (13) are solved for the new stress state assuming an elastic deformation, i. e., $d\varepsilon_r^p = d\varepsilon_\theta^p = d\varepsilon_z^p = 0$.
3. A new yield surface is computed for the present temperature at all stations.
4. Effective stress is compared to this new yield surface for each station.
5. If the effective stress is less than the effective stress at all nodes the plasticity subroutine is bypassed to go to the next thermal and mechanical load increments. Otherwise a nonzero plastic strain increment is assumed.
6. The linear system of equations (Eqn. 17), with the assumed plastic strain increment, are solved for the radial and hoop stresses. The axial stress is computed from these stresses.
7. The modified total strains and the equivalent total strain are computed from Eqs. 24 and 29, respectively.
8. The effective incremental plastic strain is computed from Eqn. 20 and the new incremental plastic strains are computed from the plastic strain-total strain relations (Eqn. 28).
9. These strains are then compared with the previous plastic strain increments and if the difference is less than a specified tolerance, go to step 1. Otherwise the linear system of equations (Eqs. 17) are solved with the new incremental plastic strains.
10. Steps 6-9 are repeated until convergence of the incremental plastic strains is obtained.

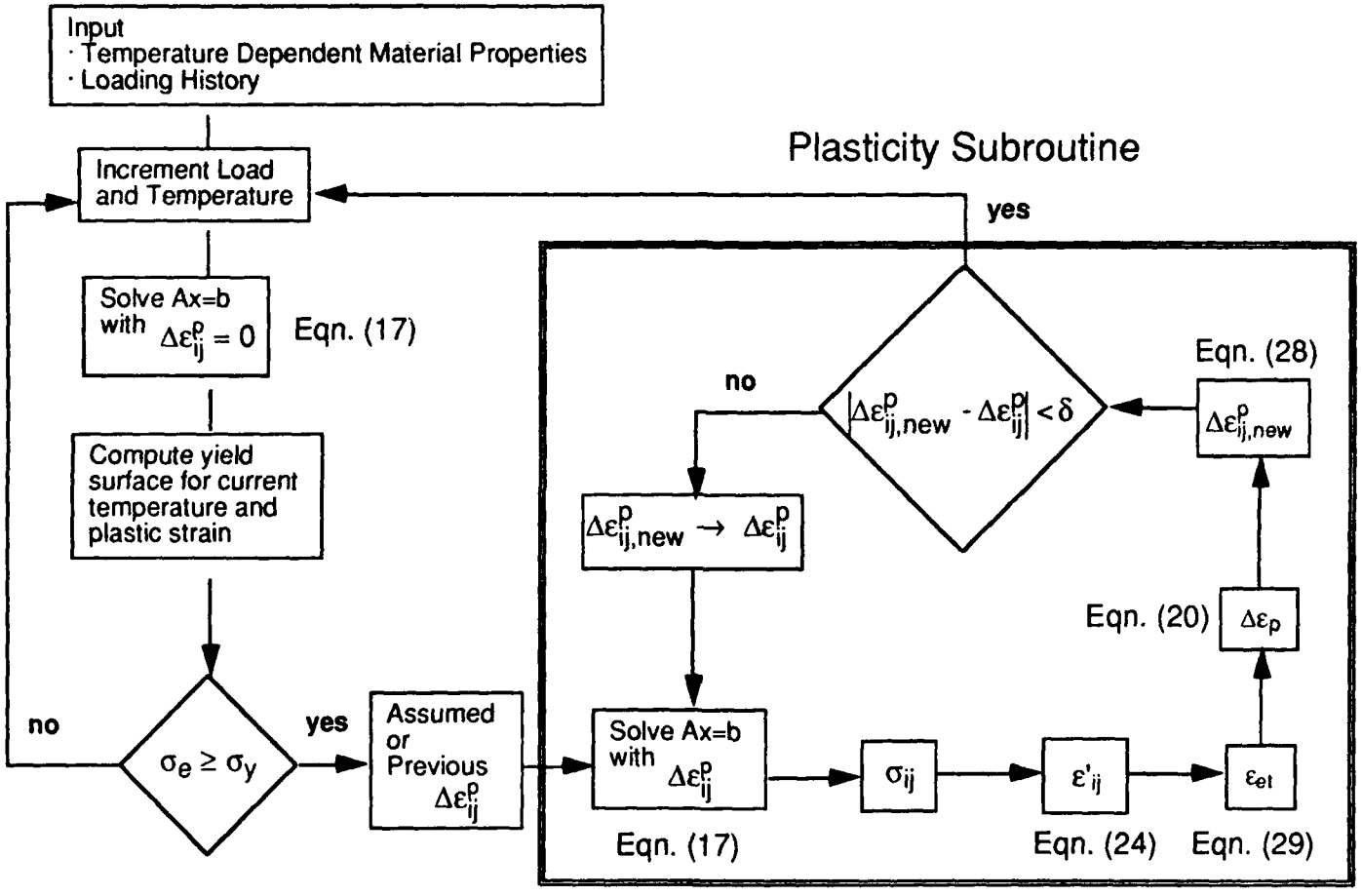

Figure 4.1 Elastic-Plastic Algorithm Used in FIDEP.

PROGRAM FIDEP

Open files
Read temperatures and loads
Read temperature dependent material data
Read geometry and create mesh
Print header lines

LOOP 1: Do for each cycle ICYC=1,NLOAD-1
  NSTEPS=NOT(ICYC+1)-NOT(ICYC)
  Loading: Divide into n steps and compute intermediate properties
  LOOP 1.1: Do ILK=2,NSTEPS+1
    Rename properties for each node at temperature
    Assume dep-new=0 and solve equations elastically
    CALL SOLVE
    CALL PLSTRAIN
    Print output: OUTS.DAT and OUTE.DAT
  Continue LOOP 1.1
  Print output: OUTSUM.DAT
Continue LOOP 1
Print output: OUTUSP.DAT
STOP

Figure 4.2 Pseudo-Code for the Computer Program FIDEP.

SUBROUTINE SOLVE

- Input assumed or estimated plastic strains
- Compute a modified axial strain without the radial stress contribution at the interface,

$$\varepsilon_z^* = \frac{\sigma_z^{app}}{E_c} + \frac{\alpha_c \Delta T}{E_c} + \frac{2}{b^2}\frac{E_m}{E_c}\int_a^b \varepsilon_z^p r dr$$

- Compute the coefficients for the finite difference equations
- Create the matrix A and the vector B with current plastic strain increments
- Solve the linear system Ax = B for the radial and hoop stresses,

$$\sigma_r(i)\ ,\ i = 1,...,NTOT\ ,\ \sigma_\theta(i)\ ,\ i = 2,...,NTOT+1$$

- Boundary conditions:

$$\sigma_r(ntot+1) = 0 \quad \text{and} \quad \sigma_\theta(1) = 0$$

- Compute axial strain:

$$\varepsilon_z = \varepsilon_z^* - 2\frac{V_f}{E_C}(\upsilon_f - \upsilon_m)\sigma_r(int+1)$$

- Compute axial stress from the axial stress-strain relationship
- Compute effective stress
- Compute strains
- RETURN

SUBROUTINE PLSTRAIN

Compute new yield surface after strain hardening for each node:

$$\sigma_e = \frac{E_p}{1 - E_p/E}\varepsilon_p^{eff} + \sigma_y$$

If $s_{eff} > s_e$ at any node go to 10 else return

[10] LOOP 2: Iterations on e_p do 1 thru 12 iterations

LOOP 2.1: Do for each node in the matrix: I=INT+1, NTOT+1

$$\sigma_e = \frac{E_p}{1 - E_p/E}\varepsilon_p^{eff} + \sigma_y$$

Define $F = \sigma_{eff} - \sigma_e$ (at node *i*)

If F>0 goto 20

else goto LOOP 2.1

[20] Compute modified total strains

Compute effective modified total strain

$$d\varepsilon_p = \frac{\varepsilon_p^{eff} - \sigma_y/3G}{1 + H/3G} \text{ where } H = \frac{E_p}{1 - E_p/E}$$

Use modified Prandtl-Reuss relations to compute incremental plastic strains; $d\varepsilon_{rp}, d\varepsilon_{\theta p}, d\varepsilon_{zp}$

Compute new plastic strains; $\varepsilon_{rp}^{(2)} = \varepsilon_{rp} + d\varepsilon_{rp}$ etc.

Continue LOOP 2.1

CALL SOLVE with $\varepsilon_p^{(2)}$

Faster Convergence Scheme

Continue LOOP 2

$\varepsilon_p = \varepsilon_p^{(2)}$

$\varepsilon_p^{eff} = \varepsilon_p^{eff} + d\varepsilon_p$

RETURN

Figure 4.2 Pseudo-Code for the Computer Program FIDEP (Continued).

4.2 Faster Convergence Scheme

To reduce the number of iterations, a faster convergence scheme was adopted [24]. In this method the three previous plastic strain increment estimates and their differences are saved and extrapolated to a plastic strain increment that would result in a difference of zero. In Fig. 4.3, the slope of the line is calculated and the new strain is obtained as -b/a, which is the y-intercept of the plastic strain vs. the difference graph.

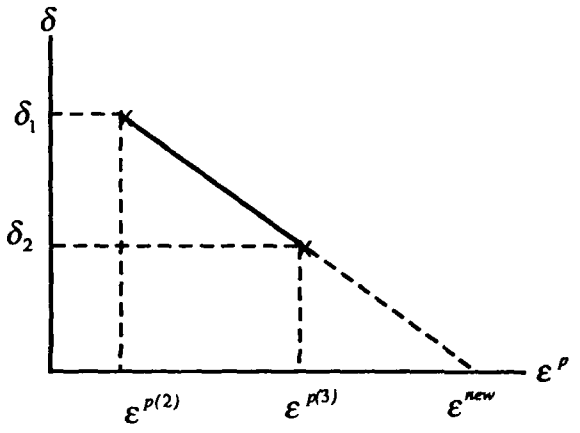

$$\delta = a\varepsilon^p + b$$

$$\delta_1 = \varepsilon^{p(2)} - \varepsilon^{p(1)}$$

$$\delta_2 = \varepsilon^{p(3)} - \varepsilon^{p(2)}$$

$$\varepsilon^{new} = -\frac{b}{a}$$

where

$$a = \frac{\delta_2 - \delta_1}{\varepsilon^{p(3)} - \varepsilon^{p(2)}} = 1 - \frac{\delta_1}{\delta_2}$$

$$b = \delta_2 - a\varepsilon^{p(3)}$$

Figure 4.3 Schematic for the Computation of a New Estimate for the Plastic Strains Using the Previous Estimates and their Differences.

CHAPTER 5
PROGRAM

5.1 General Description

FIDEP (Finite-Difference Code for Elastic-Plastic Analysis) is a user-friendly computer program designed to solve the problem of concentric cylinders subjected to thermal and mechanical loading. The program is simple in structure and scope since it was intended to be used as a practical research tool for the determination of stress concentrations in the matrix around the fiber in unidirectional continuous fiber reinforced metal matrix composites. The features of the program include:

- generalized plane strain and axisymmetric geometry,
- small displacements,
- isotropic and incompressible fiber and matrix,
- elastic fiber and time-independent bilinear elastic-plastic matrix (including perfectly plastic matrix),
- perfect bonding between the fiber and the matrix,
- uniform temperature change throughout the composite.

More advanced features such as time-dependent material behavior, multiple concentric cylinders are absent from the current version of the program since only speedy prediction of the time-independent nonlinear behavior of a two-phase unidirectional composite was required at the time.

Operation of FIDEP program is straightforward, requiring the modification of a loading history file and a material properties data file. All input data are in free format and some descriptive titles are allowed. The following sections describe the operation of the program.

5.2 Program Operation

The execution of the program consists of changing two input files and executing the code. The input files are the loading history file, FDLOAD.DAT, and temperature-dependent constituent property data file, FDMAT.DAT. Running the code creates four output files:

FDOUTS, FDOUTE, FDUSP, FDSUM. The first two files consist of the stress and strain history, respectively, of the matrix at the interface. The output file FDUSP consists of the stress-strain distribution that exists in the composite at the end of the imposed loading history. The output file FDSUM consists of a summary of the fiber and matrix stresses at the interface at the end of each half-cycle. In the following sections the input and output file formats are explained in detail.

5.2.1 Input

The input consists of two files: loading file and material properties file. The loading file data specifies the number of steps, temperature, and applied mechanical stresses and the second file specifies the temperature dependent mechanical properties for the constituents.

The loading file, FDLOAD, format is listed in Table 5.1. An example loading history data file for cyclic loading at room temperature after cooldown from processing is shown in Fig. 5.1.

The material property data specifies the following properties for the matrix and the fiber: elastic modulus, coefficient of thermal expansion, Poisson's ratio, yield stress and plastic modulus for each temperature. The material data file, FDMAT, format is listed in Table 5.2. An example material data file for SCS-6 fiber and Ti-24Al-11Nb matrix material is shown in Fig. 5.2.

5.2.2 Output

There are four output files: FDOUTS.DAT, FDOUTE.DAT, FDUSP.DAT and FDSUM.DAT. The first two files contain stresses and strains, respectively, in the matrix at the fiber/matrix interface at each step increment. FDUSP.DAT contains the stresses and strains along the radius for the final loading step. FDSUM.DAT contains a summary of the stresses and strains at the interface in the fiber and the matrix at the end points of each cycle. The runtime is printed on the screen at the completion of the program. The output formats are described in the following paragraphs.

FDOUTS.DAT echos the inputs from the loading and material data files at the beginning of the file. Following the input, the stresses and the mechanical strain in the matrix computed at the fiber/matrix interface are printed in the following order: computational step, and

```
Cooldown and Mechanical Cycling at Room Temperature
Comment line 2
Comment line 3
Comment line 4
5
0          30    60    90    120   0     0     0     0
1010 25    25    25    25    0     0     0     0
0          0     350   35    350   0     0     0     0
```

Figure 5.1 Example Loading History Input File, FDLOAD.DAT.

```
TI-24-11 Matrix and SCS-6 Fiber Properties
Comment line 2
2
11
TEMP  E(GPa) CTE(1E-6/C)      MU    SY(MPa)  EP(GPa)
20    413    4.72          0.3    1.E6          0.
101   413    4.81          0.3    1.E6          0.
203   413    4.96          0.3    1.E6          0.
299   413    5.09          0.3    1.E6          0.
400   413    5.23          0.3    1.E6          0.
500   413    5.36          0.3    1.E6          0.
598   413    5.44          0.3    1.E6          0.
702   413    5.51          0.3    1.E6          0.
800   413    5.66          0.3    1.E6          0.
900   413    5.73          0.3    1.E6          0.
1010  413    5.75          0.3    1.E6          0.
8
TEMP  E(GPa) CTE(1E-6/C)       MU    SY(MPa)  EP(GPa)
20    84.10 11.33 0.3    950.0 0.00
315.  88.40 11.88 0.3    410.0 3.29
482.2       68.26 12.22 0.3    333.3 3.71
649.0       48.09 12.73 0.3    256.5 4.12
704.4       42.08 12.95 0.3    214.1 3.89
760.0       36.07 13.22 0.3    171.8 3.67
885.0       23.66 13.93 0.3    112.8 3.91
1010.0      11.25 14.97 0.3     53.8 4.15
Reference Temperature
1010
 Vf     b
0.35        1.0
```

Figure 5.2 Example Material Properties Input File, FDMAT.DAT.

Table 5.1 Format for the Loading Data File, FDLOAD.DAT.

Card	Column	Variable	Definition
1-4			Comment lines
5	1	NLOAD	Number of columns of loading data to be read
6	1-NLOAD	NOT	Step number
7	1-NLOAD	TE	Temperatures (°C) corresponding to step NOT
8	1-NLOAD	PAT	Applied axial stresses (MPa) corresponding to step NOT

Table 5.2 Format for the Material Properties File, FDMAT.DAT.

Card	Column	Variable	Definition
1-2			Comment lines
3	1	NOMAT	Number of constituents (1)
4	1	NROW	Number of rows of material property data for the first constituent following header line
5	1		Header line for the properties
6	1	TEMP	Temperature (°C)
	2	EMAT	Modulus (GPa)
	3	CTEMAT	Coefficient of thermal expansion (E-6/°C) (2)
	4	MUMAT	Poisson's ratio
	5	SYMAT	Yield stress (MPa) (3)
	6	EPLMAT	Plastic modulus (GPa) (4)
7 -			Repeat cards 4-6 for the matrix
8			Comment line
9	1	TREF	Reference temperature (5)
10			Comment line
11	1	VF	Fiber volume fraction
	2	B	Outer radius of matrix (usually 1.0)

Notes: (1) The number of constituents is limited to two at the present.

(2) Secant coefficient of thermal expansion (CTE) is used. The reference temperature for the secant CTE should be the initial processing temperature.

(3) (4) For the fiber, artificially high value is given for the yield stress and zero value is given for the plastic modulus since the fiber is assumed to be elastic.

(5) This is the same temperature as the initial processing temperature used in loading history data file.

corresponding temperature, applied axial stress, effective stress, radial stress, hoop stress, axial stress, original yield surface, and axial strain. The column titles are shown below.

Step Temp σ_{app} σ_{eff} σ_r σ_θ σ_z Y. S. ε_z

The stresses are given in units of MPa, temperature in °C, and the strain in mm/mm. The effective stress is defined by:

$$\sigma_{eff} = \sqrt{1/2\left[(\sigma_r - \sigma_\theta)^2 + (\sigma_r - \sigma_z)^2 + (\sigma_z - \sigma_\theta)^2\right]}$$

which is equivalent to Eqn. 20.

FDOUTE.DAT consists of the strains in the matrix at the fiber/matrix interface in the following order: computational step, and corresponding temperature, applied axial load, radial plastic strain, hoop plastic strain, axial plastic strain, radial mechanical strain, hoop mechanical strain, axial mechanical strain and thermal strain. The column titles are shown below:

Step Temp s_{app} ε_r ε_θ ε_z ε_{rme} $\varepsilon_{\theta me}$ ε_{zme} ε_{th}

FDUSP.DAT consists of the stresses and plastic strains across the cross section of the composite at the end of loading history in the following order: radius, effective stress, radial stress, hoop stress, axial stress, radial plastic strain, hoop plastic strain and axial plastic strain. The column titles are shown below:

Radius σ_{eff} σ_r σ_θ σ_z ε_{rp} $\varepsilon_{\theta p}$ ε_{zp}

FDSUM.DAT consists of a summary of the stresses and strains at the interface in the fiber and matrix at the end points of each loading/unloading cycle in the following order: step number corresponding to steps in the loading file, FDLOAD, temperature, applied stress, axial fiber stress, axial matrix stress, effective matrix stress, effective matrix strain and axial mechanical strain in the matrix. The column titles are shown below:

Step Temp σ_{app} σ_z^f σ_z^m σ_{eff}^m ε_{eff}^m ε_{zme}^m

5.2.3 Program

The program FIDEP is listed in Appendix A. The program uses a default value of 50 divisions in the cylinders for applying the finite difference method. These finite difference equations result in a linear system of 100 equations in 100 unknowns represented by the variable NRA in the program. If a better accuracy is desired NRA can be changed to 200 in the subroutine SOLVE.

5.2.4 Execution of FIDEP on a VAX/VMS Machine

The program FIDEP can be run interactively or in a batch mode on a VAX-VMS machine and requires IMSL library of subroutines [27]. Before execution, the program is compiled and linked on a VAX/VMS machine as follows:

> FOR FIDEP
> LINK FIDEP+IMSL/LIB
To run FIDEP in real time type
> RUN FIDEP

To run FIDEP on a batch mode a command file has to be created. In this command file the input and output files can be renamed. An example command file is shown in Fig. 5.3. This command file is then submitted to the batch using the command

> SUBMIT/NOPRINT filename

After the job has been completed a log file will appear in the main directory.

```
$     SET VERIFY
$     ASSIGN/USER_MODE [COKERDU.FIDEP]FDMAT.DAT FDMAT
$     ASSIGN/USER_MODE [COKERDU.FIDEP]FDLOAD.DAT FDLOAD
$     ASSIGN/USER_MODE [COKERDU.FIDEP]FDOUTS.DAT FDOUTS
$     ASSIGN/USER_MODE [COKERDU.FIDEP]FDOUTE.DAT FDOUTE
$     ASSIGN/USER_MODE [COKERDU.FIDEP]FDUSP.DAT FDUSP
$     ASSIGN/USER_MODE [COKERDU.FIDEP]FDSUM.DAT FDSUM
$     RUN [COKERDU.FIDEP]FIDEP3B
```

Figure 5.3 Example Command File for Running Batch Jobs on a VAX/VMS Machine.

CHAPTER 6
DEMONSTRATION PROBLEMS

Several problems are solved using FIDEP code to illustrate the capability for computing micromechanical stresses and to compare with solutions obtained by other methods. The first case is the comparison of FIDEP solution to the closed form solution for an elastic problem. The second case is the comparison of FIDEP results with finite element analysis results for thermal cool-down and thermal cyclic loading. The third case is an application problem in which the stresses and strains are predicted in a unidirectional composite subjected to in-phase and out-of-phase thermomechanical fatigue behavior and the strains are compared with experimental measurements.

6.1 Material Properties

In these computations two-material concentric cylinder model consisting of SCS-6 silicon carbide fiber and Ti-24Al-11Nb matrix is used. The mechanical properties for SCS-6 and Ti-24Al-11Nb are shown in Table 6.1 as a function of temperature. The SCS-6 fiber is isotropic and elastic with only the coefficient of thermal expansion varying with temperature. An adequate representation of the Ti-24Al-11Nb matrix was attained using a bilinear elastic-plastic model with temperature dependent elastic and plastic moduli, yield stress and coefficient of thermal expansion.

6.2 Comparison with an Elastic Solution

An elastic closed form solution for two concentric cylinders and generalized axisymmetric condition is presented in Appendix 2 [28]. The stresses at the cross-section obtained by FIDEP and by the closed form solution for ΔT=-100°C is shown in Fig. 6.1. In this analysis temperature independent elastic properties were used with the following properties: E_f = 414 GPa, ν_f = 0.22, α_f = 4.7E-6 /°C, E_m = 90 GPa, ν_m = 0.30, α_m = 10.7E-6 /°C, where f denotes the fiber and m denotes the matrix. The fiber volume fraction was 35%. The stresses obtained by the two method are in excellent agreement as shown in Fig. 6.1.

Stresses at the cross-section using the elastic-plastic and the elastic solution is compared in Fig. 6.2 using the mechanical properties from Table 6.1. The temperature

Table 6.1 Mechanical Properties for SCS-6 Fiber and Ti-24Al-11Nb Matrix.

SCS-6 Fiber Properties
$\nu = 0.22$
E = 414 GPa

Temperature (°C)	α * (10^{-6}/°C)
20	4.70
93	4.81
204	4.97
316	5.12
427	5.26
538	5.38
649	5.50
760	5.60
871	5.70
982	5.78
1010	5.80

Ti-24Al-11Nb Matrix Properties
$\nu = 0.22$

Temperature (°C)	α * (10^{-6}/°C)	Elastic Modulus (GPa)	Yield Stress (MPa)	Plastic Modulus (GPa)
20	12.33	94	604	1.3
93	12.47	92	560	0.9
204	12.78	91	498	0.7
316	13.21	89	447	0.7
427	13.75	79	421	0.4
538	14.42	70	381	0.1
649	15.20	50	357	0
760	16.10	25	252	2.3
871	17.11	18	138	2.6
982	18.25	16	38	1.2
1010	18.55	15	30	1.0

* α is secant coefficient of thermal expansion with a reference temperature of 1010°C.

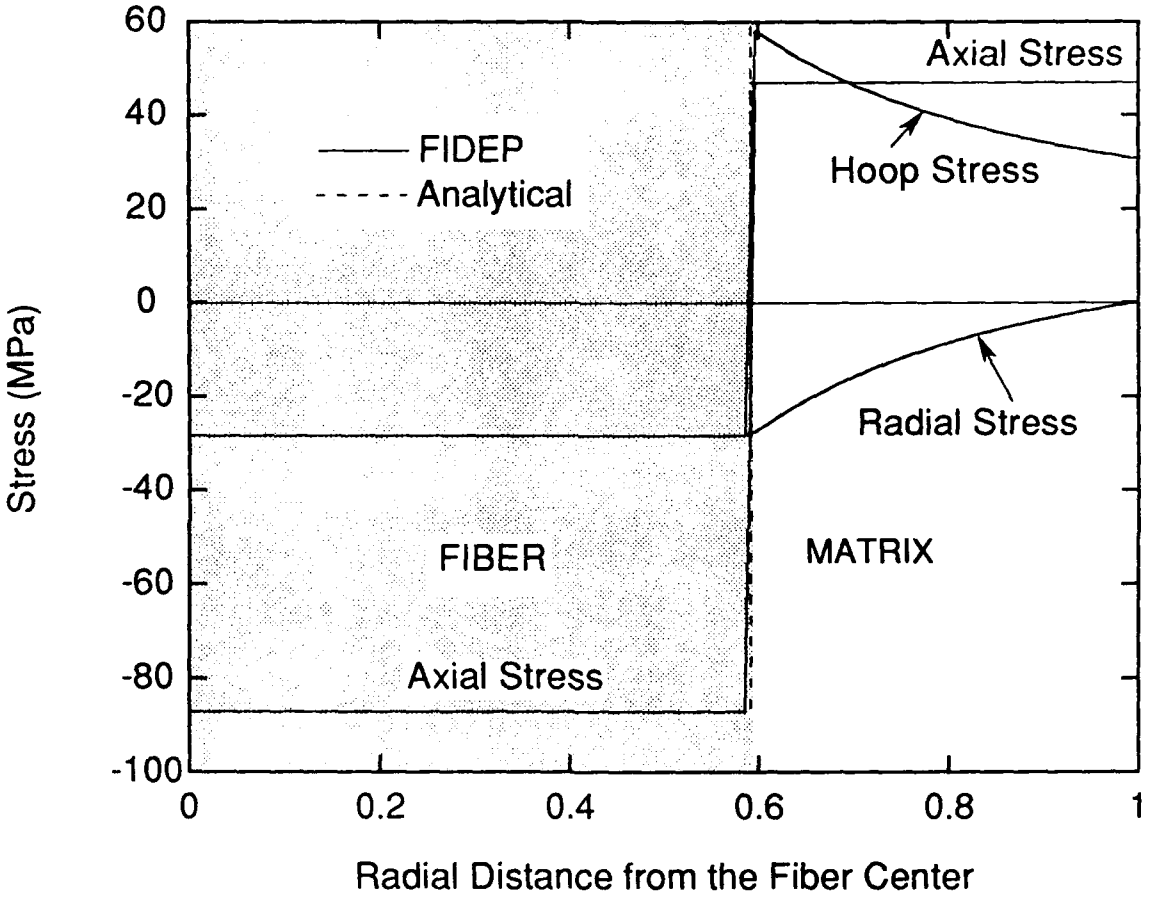

Figure 6.1 Variation of Elastic Stresses with Radius Obtained by Elastic Closed-Form Solution and FIDEP for $\Delta T = -100°C$.

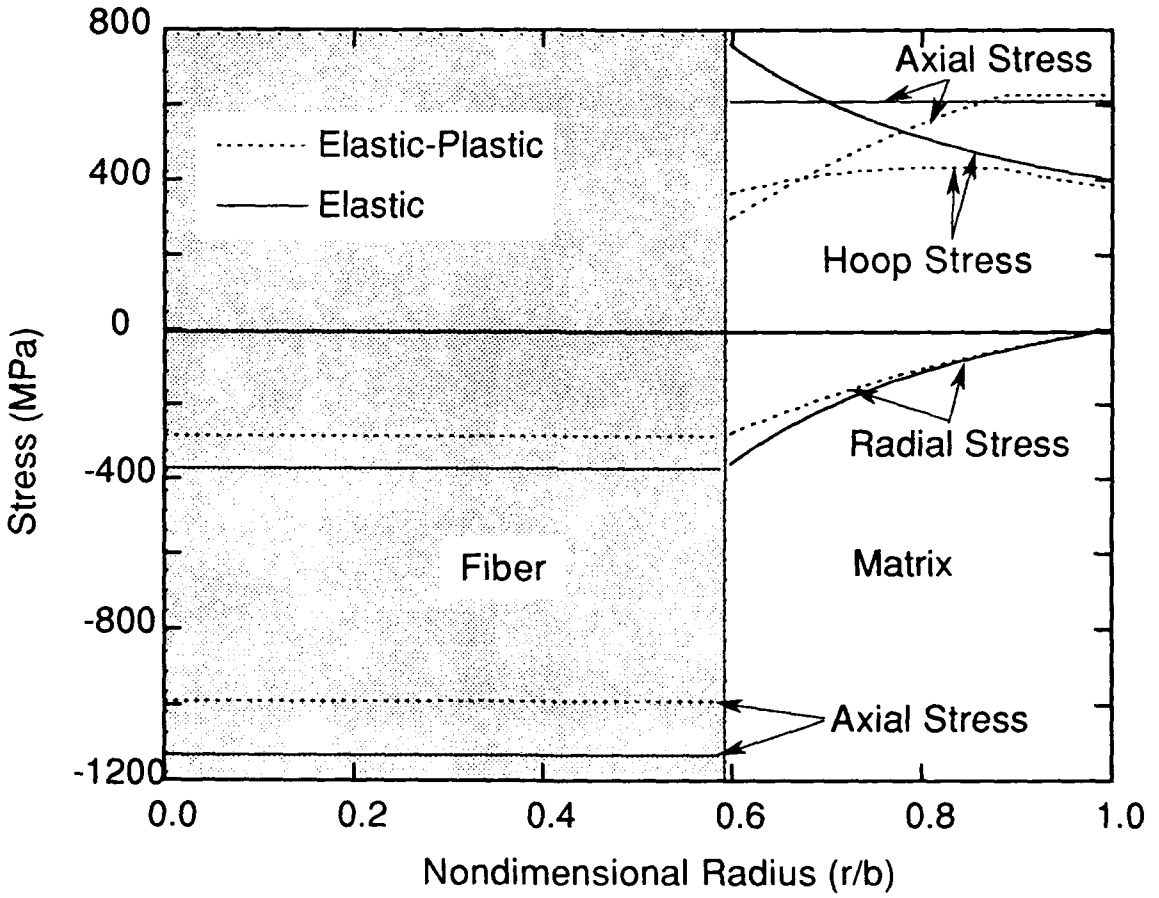

Figure 6.2 Variation of the Stresses Across the Cross-Section of the CCM After Cool-Down from Processing Temperature of 1010°C for Elastic and Elastic-Plastic Matrix.

dependent elastic solution was obtained from FIDEP by making the yield stress artificially high (1.E6 MPa) for the matrix. The loading input file and a schematic of the loading history is shown in Fig. 6.3. The yield surface is first reached at the interface and the matrix near the interface becomes plastic. As the thermal loading increase the plastic zone spreads outwards to the rest of the matrix and a redistribution of the stresses occur. In the elastic region, the radial and hoop stresses change proportional to $1/r^2$ and the axial stress remain uniform. Inside the plastic zone, the radial and hoop stresses remain almost uniform and the axial stress decreases when the effective stress cannot extend beyond the yield stress. The remaining load is redistributed to the fiber and the elastic region of the matrix.

6.3 Comparison with Finite Element Method

Two examples are presented and the results from FIDEP are compared with finite element method (FEM) results obtained from nonlinear finite element code MAGNA [29]. The temperature dependent plasticity subroutines were implemented in MAGNA by J. L. Kroupa [30]. The geometry and the boundary conditions for the finite element model of an axisymmetric concentric cylinder geometry under generalized plane strain condition are shown in Fig. 6.4 [30]. Contact elements were used to model the fiber-matrix interface, which allowed the separation of the fiber and matrix when the matrix stresses at the interface became positive. Isotropic hardening model with a bilinear elastic-plastic stress-strain curve was used to model the matrix. The fiber was elastic and the volume fraction was 35%. The material properties listed in Table 6.1 were used for the analysis.

6.3.1 Cool-Down from Processing Temperature

The first comparison problem with FEM was the thermal cool-down associated with processing the material. The loading input file and a schematic of the loading history is shown in Figure 6.3. The fiber and matrix are assumed to have zero stresses and strains at the initial consolidation temperature of 1010°C. As the material cools down, the modulus changes with temperature and the difference in coefficient of thermal expansion between the fiber and matrix leads to thermal stresses in the fiber and matrix. The material properties are those shown in Table 6.1. The output from the program is presented in Appendix C. The files FDOUTS.DAT and FDUSP.DAT were used in Figs. 6.5-6.8 discussed below.

The three-dimensional stresses computed during the cool-down process are illustrated in Fig. 6.5. The computed stresses, shown as the dashed lines with symbols in

Loading File 1
Cool-Down to Room Temperature
From a Processing Temperature of 1010°C
For SCS-6/Ti-24Al-11Nb Unidirectional Composite
2
0 30
1010 20
0 0

(a)

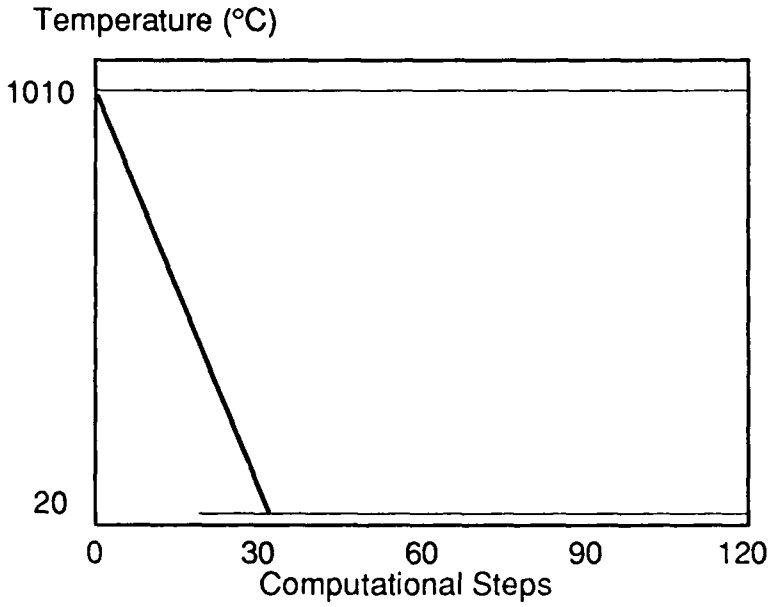

(b)

Figure 6.3 a) Loading Input File, and b) Schematic of the Temperature History for a Thermal Cool-Down Simulation of SCS-6/Ti-24Al-11Nb Unidirectional Composite.

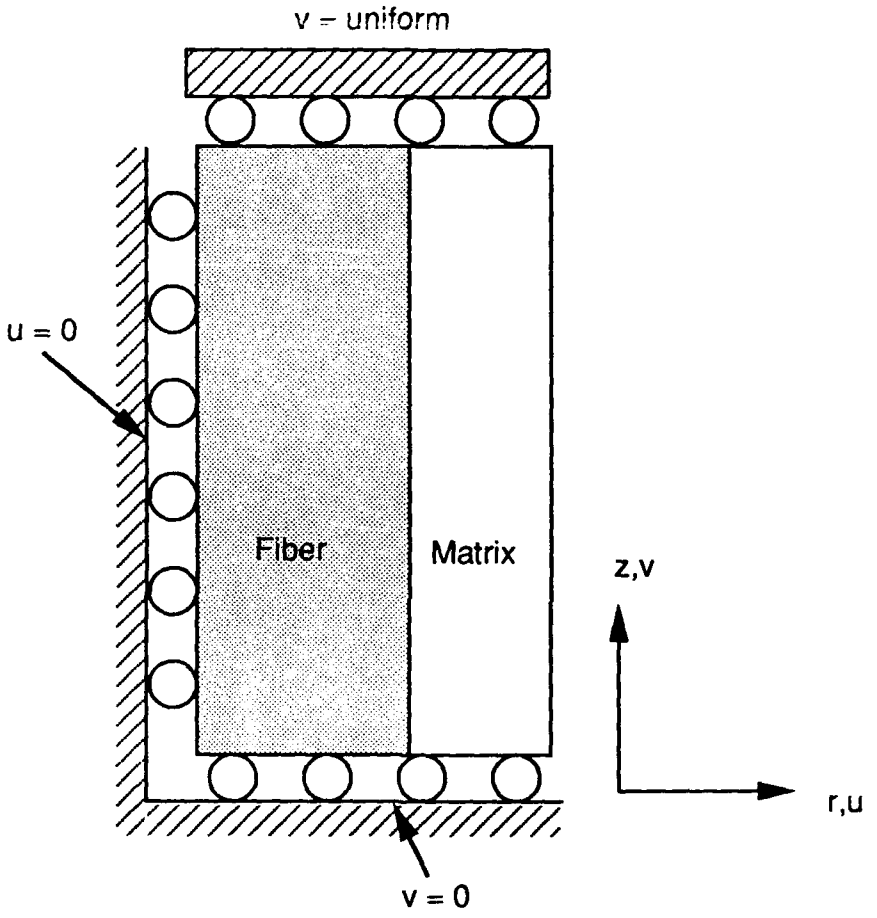

Fig. 6.4 Finite Element Model and the Boundary Conditions for an Axisymmetric Concentric Cylinder Geometry Under Generalized Plane Strain Condition.

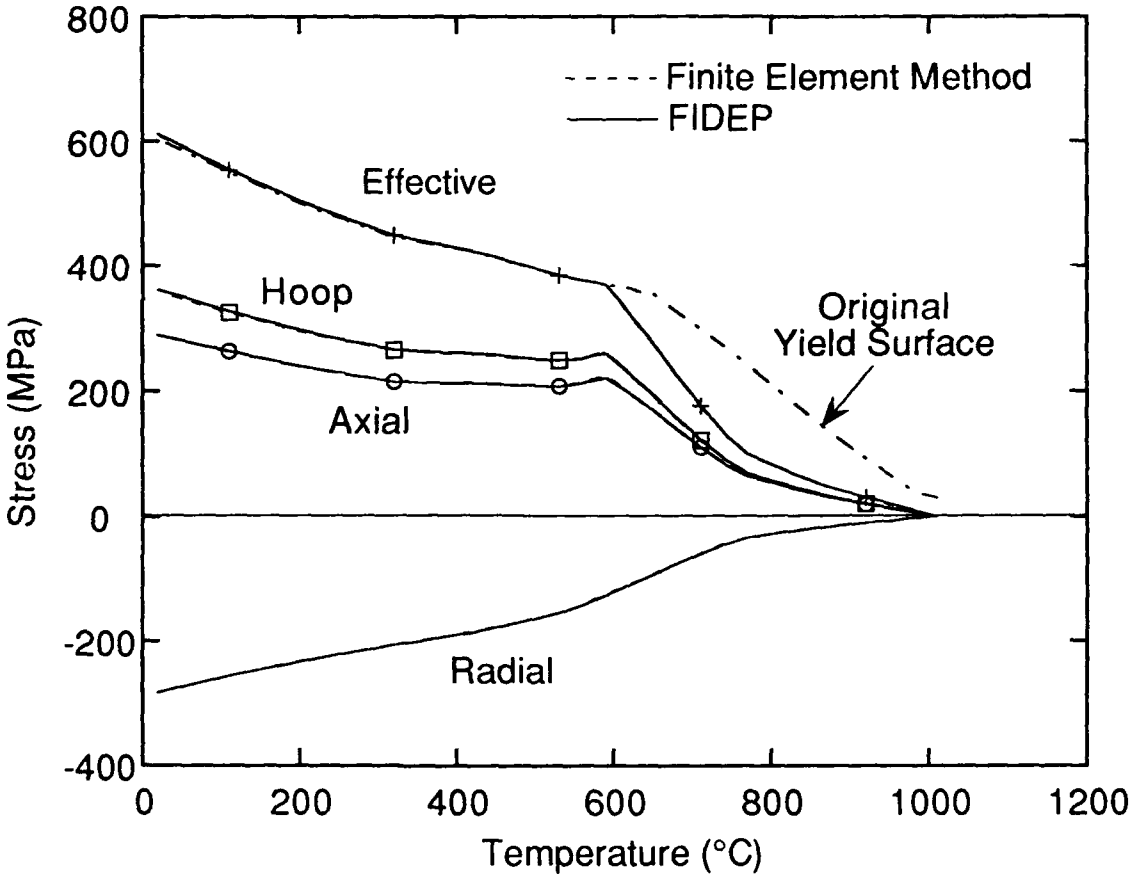

Figure 6.5. Finite Element and FIDEP Predictions for the Stresses at the Interface in Ti-24Al-11Nb Matrix After Cool-Down from Processing Temperature of 1010°C.

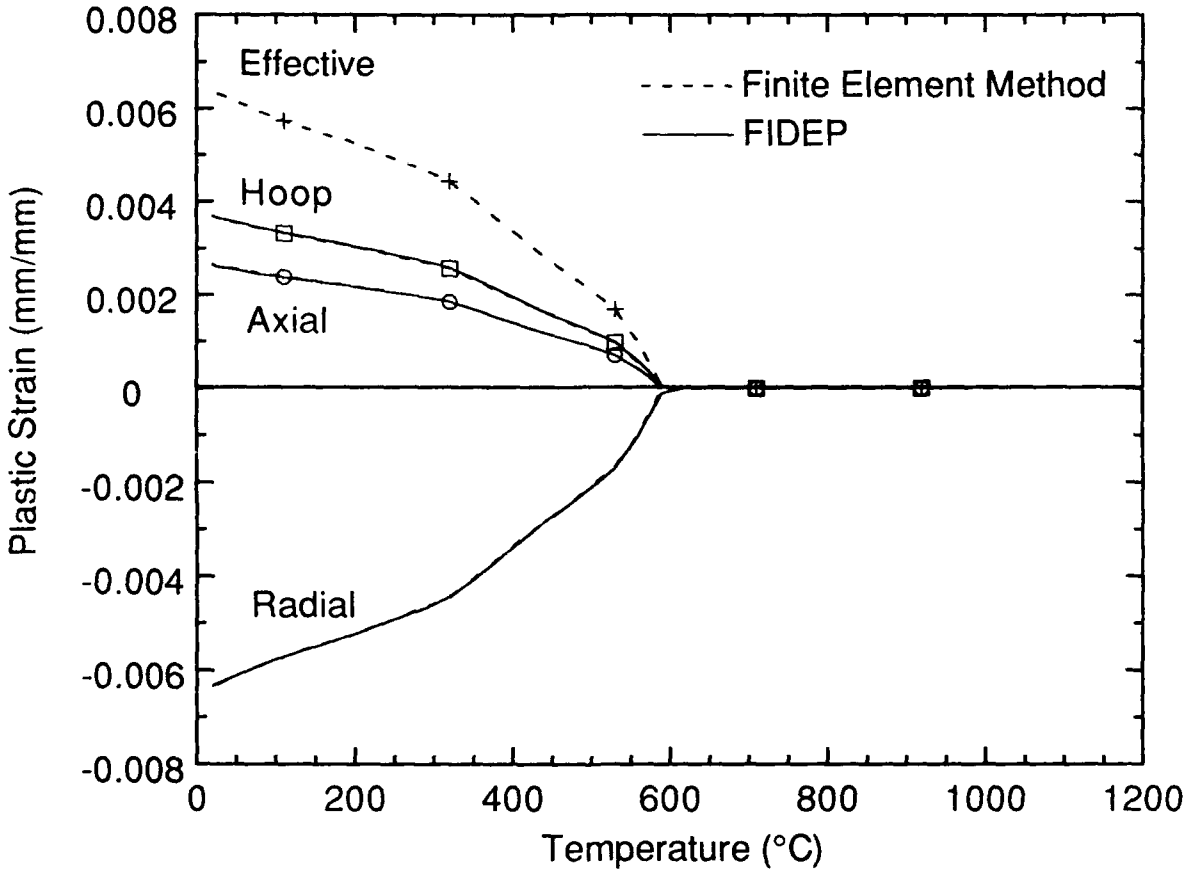

Figure 6.6 Finite Element and FIDEP Predictions of the Plastic Strains in Ti-24Al-11Nb Matrix at the Fiber-Matrix Interface After Cool-Down from Processing Temperature of 1010°C.

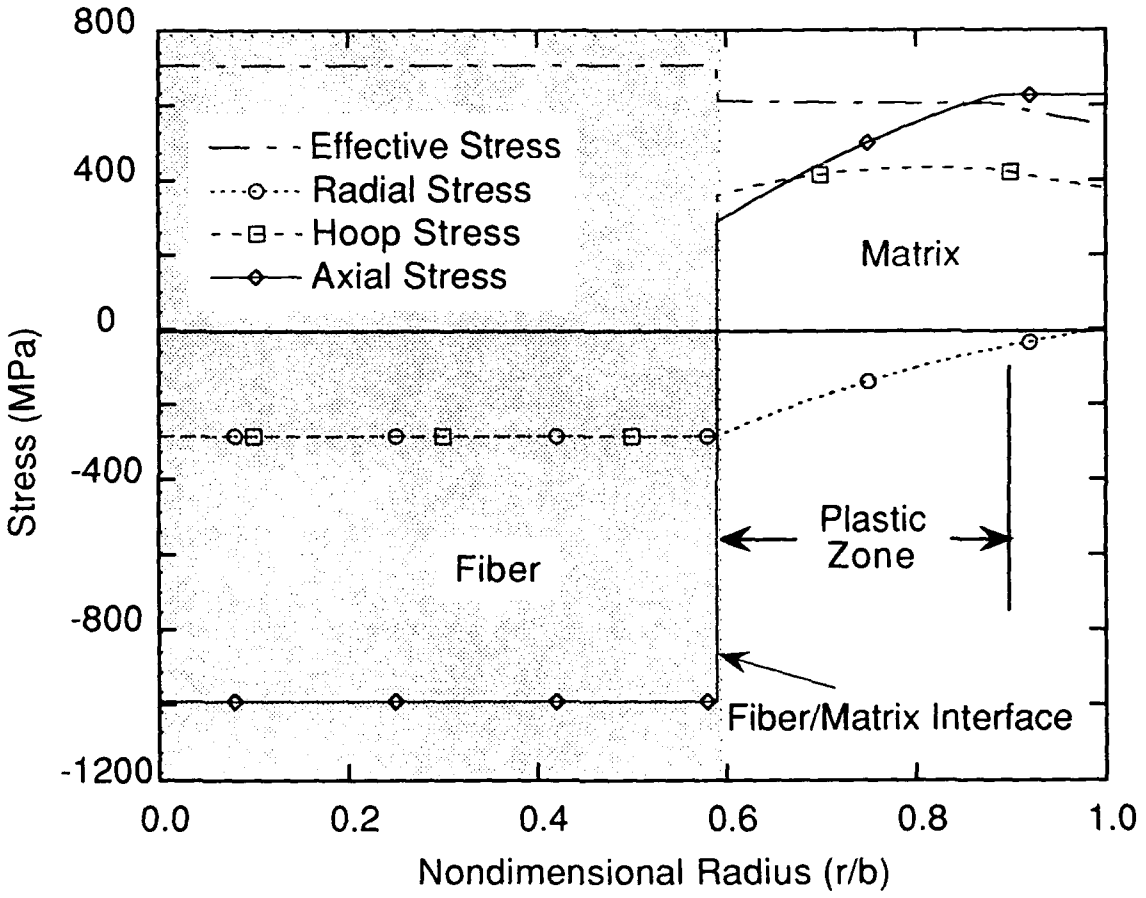

Figure 6.7 Variation of the Stresses Across the Cross-Section of the CCM After Cool-Down from Processing Temperature of 1010°C.

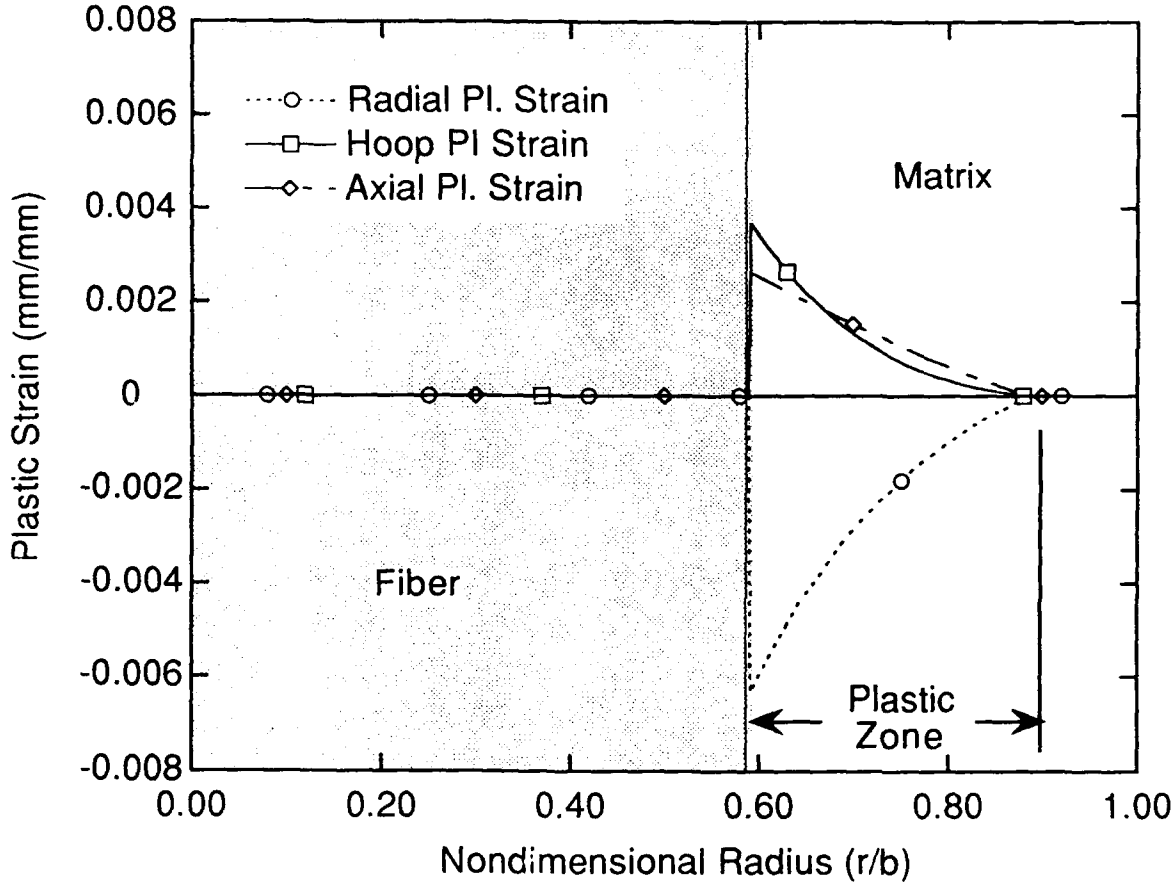

Figure 6.8 Variation of the Plastic Strains Across the Cross-Section of the CCM After Cool-Down from Processing Temperature of 1010°C.

the plot, are compared with results for the same problem solved by FEM represented by the solid lines. The agreement with the finite element results is excellent. The computations show that the matrix material reaches the yield surface at approximately 600°C and remains in contact with the yield surface for all lower temperatures. The axial and hoop stresses are tension and the radial stress is compressive at room temperature and of equal magnitude.

The plastic strains in the matrix at the fiber-matrix interface as a function of temperature are shown in Fig. 6.6. It can be seen here, as in Fig. 6.5, that the matrix deforms elastically until 600°C where the matrix stresses reach yield surface and start deforming plastically after which measurable plastic strains develop in the three principal directions. These results are compared with FEM computations and provide excellent agreement as shown in the figure.

Figures 6.7-6.8 display the stresses and the plastic strains at room temperature across the cross-section of the composite, respectively. The shaded areas denote the regions of plastic deformation. Plasticity initiates at the interface and propagates across the matrix with increased mechanical stress on the matrix. In this particular case, the plastic deformation has stopped at r/b=0.91 and the rest of the matrix has remained elastic. If a tensile mechanical load is superimposed at room temperature this will further propagate the plastic region until all the matrix yields.

6.3.2 Cyclic Thermal Loading

In this example the SCS-6/Ti-24Al-11Nb composite is thermally cycled between processing temperature and room temperature as shown in Fig. 6.9. The effective stress and the radial stress as a function of temperature are plotted and compared with results from FEM in Fig. 6.10. FIDEP results are in excellent agreement with finite element results prior to attaining a temperature of 850°C at the end of the first cycle. The two methods digress after 850°C because of the changing of the compressive matrix radial stresses at the interface to tensile at this temperature (Fig. 6.10). In the case of the tensile radial stress the finite element model asssumes debonding of the matrix from the fiber to occur whereas the present model assumes perfect bonding. Thus, the two methods predict different but similar states after debonding takes place.

Loading File 1
Cyclic Thermal Loading
Between Room Temperature and Processing Temperature
Temperature: 20 C to 1010 C
4

0	30	90	120
1010	20	1010	20
0	0	0	0

(a)

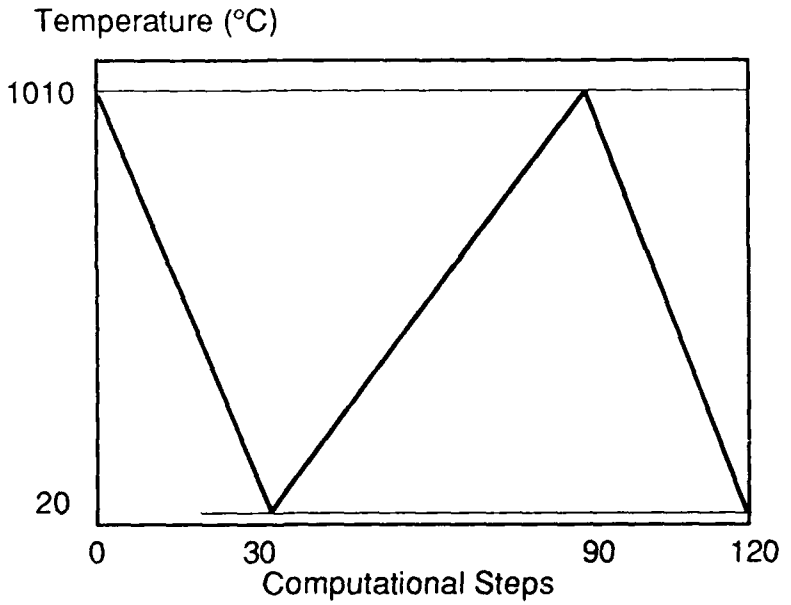

(b)

Figure 6.9 a) Loading Input File, and b) Schematic of the Temperature History for Thermal Cyclic Loading Simulation of SCS-6/Ti-24Al-11Nb Unidirectional Composite.

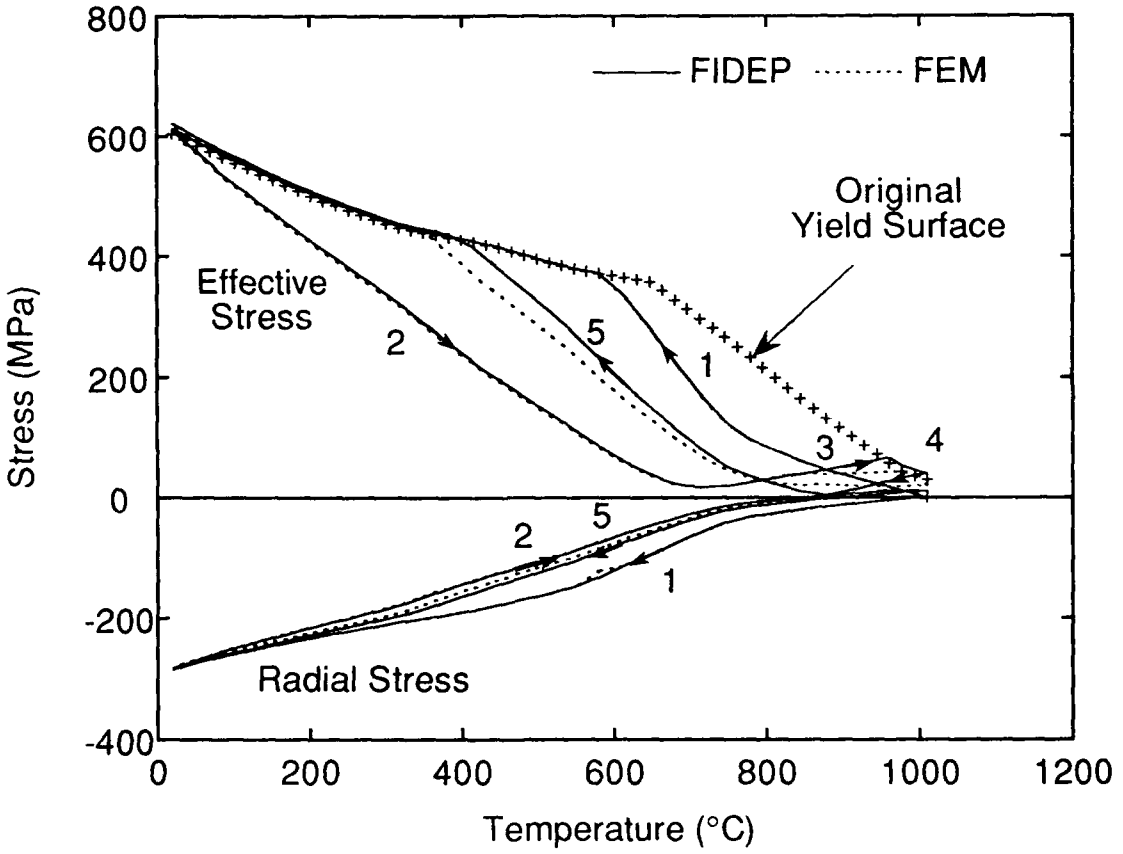

Figure 6.10 FIDEP and FEM Predictions for the Effective and Radial Stresses in the Matrix at the Fiber-Matrix Interface for Thermal Loading History shown in Fig. 6.9.

6.4 Thermomechanical Fatigue (TMF)

The FIDEP code was used to compute stresses for simulated TMF cycles to illustrate the micromechanical stresses developed during two typical TMF tests on a SCS-6/Ti-24Al-11Nb composite. The two tests are in-phase (IP) and out-of-phase (OOP) cycles and are shown schematically in Fig. 6.11. In both tests, the first part of the cycle is the cool-down from processing temperature discussed previously. This is accomplished under zero external load conditions. The horizontal axis in Fig. 6.11 represents an arbitrary time scale and is shown in terms of computational steps. Step 20 represents the room temperature condition after cool-down. The values shown in the figure correspond to TMF cycles which were evaluated experimentally and involve a maximum stress of 800 MPa, R=0.1 (ratio of minimum to maximum stress) for the OOP and IP cases, and a temperature range of 150 to 650°C.

The variation of the stresses across the cross section for an OOP cycle is illustrated in Fig. 6.12. The stresses in both fiber and matrix are shown at the minimum temperature (maximum load) in (a) while stresses at maximum temperature (minimum load) are presented in (b). At 150°C, Fig. 6.12(a) shows a large tensile axial stress in the fiber and tensile axial stresses in the matrix. The fiber stresses are essentially independent of radial coordinate, but the matrix stresses vary significantly with radius because of the complex three-dimensional stress state which arises in the concentric cylinder configuration. Matrix axial stresses are maximum at the outer radius and minimum at the fiber-matrix interface. Hoop stresses, on the other hand, are minimum at the outer radius of the cylinder but do not vary as much as the axial component. The matrix radial stress is negative at the fiber-matrix interface and goes to zero at the outer radius because of the imposed stress-free boundary condition. The stresses developed are the net result of the thermal stresses developed at a low temperature, the axial component of which is compression in the fiber and tension in the matrix, and the applied mechanical stresses which are tension in both fiber and matrix in the axial direction.

At elevated temperature in an OOP TMF cycle, the stress state is generally small as shown in Fig. 6.12(b). Under this condition, the thermal stresses are small because at high temperature the stresses are relaxed while the mechanical stresses are small because this is the condition of minimum load.

Loading File 1
Cool-Down and In-Phase TMF Loading
Load: 80 MPa to 800 MPa
Temperature: 150 C to 650 C

7						
0	30	60	90	120	150	180
1010	20	650	150	650	150	650
0	0	800	80	800	80	800

Loading File 2
Cool-Down and Out-of-Phase TMF Loading
Load: 80 MPa to 800 MPa
Temperature: 150 C to 650 C

7						
0	30	60	90	120	150	180
1010	20	650	150	650	150	650
0	0	80	800	80	800	80

(a)

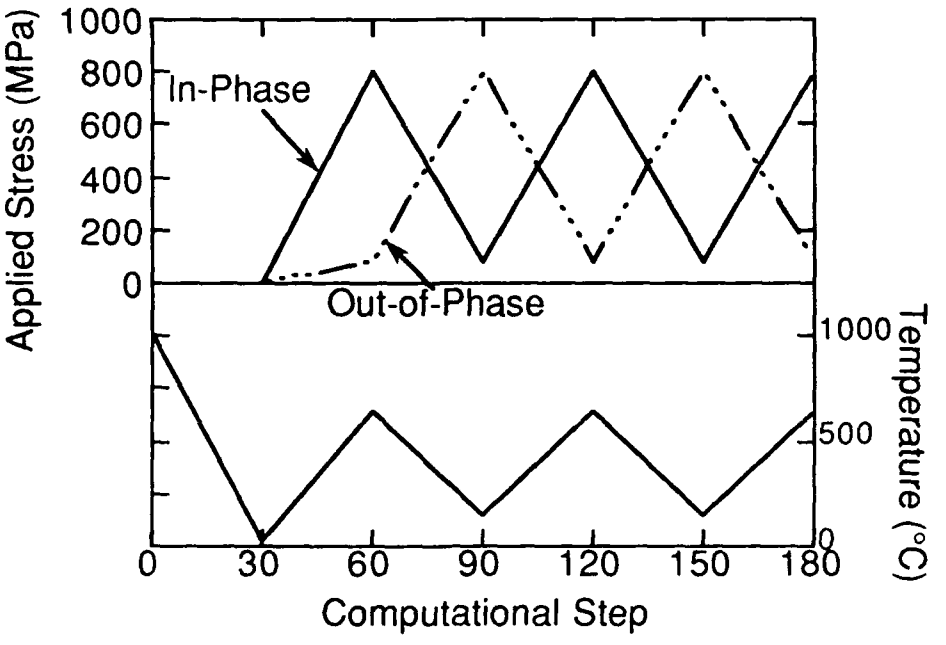

(b)

Figure 6.11 a) Loading Input Files, and b) Schematic of the Temperature and Stress History for Typical In-Phase and Out-of-Phase TMF Cycles.

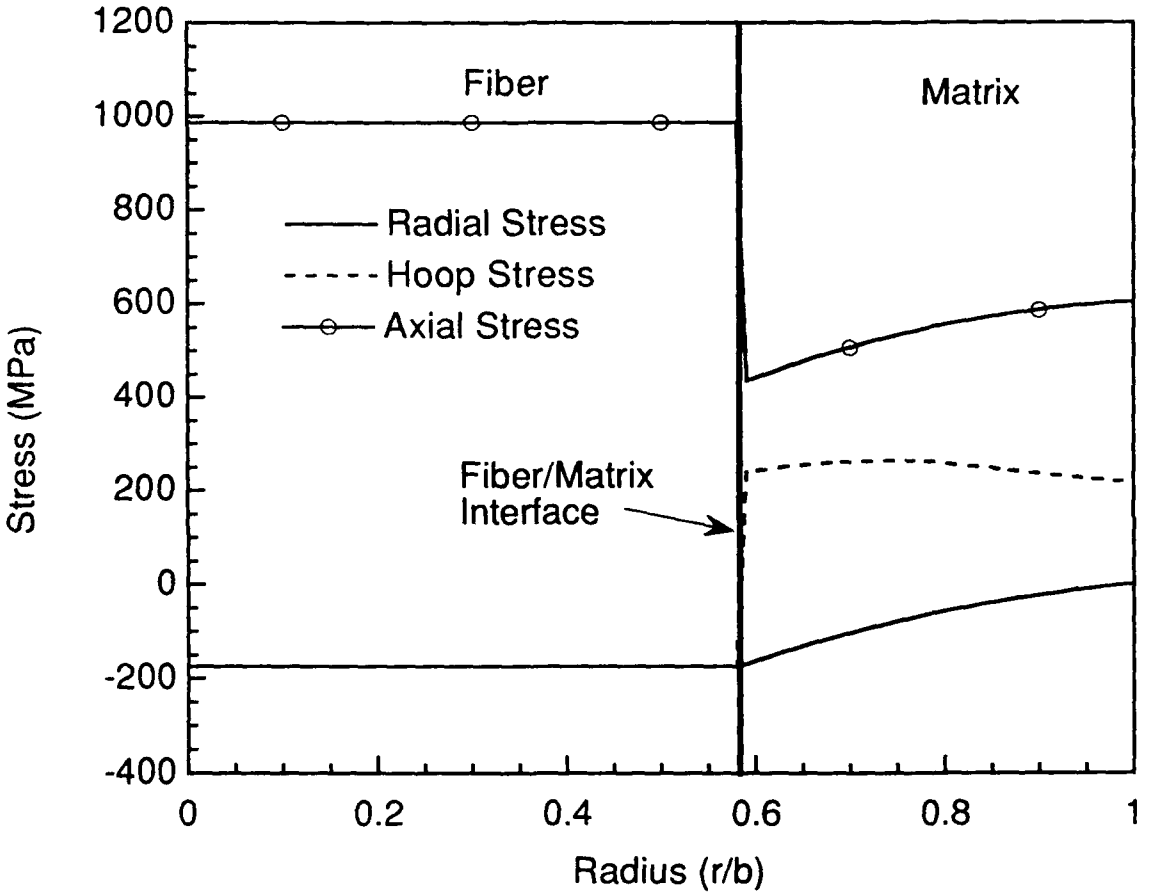

Figure 6.12a Variation of Predicted Stresses with Radius for an Out-of-Phase TMF Cycle at 150°C.

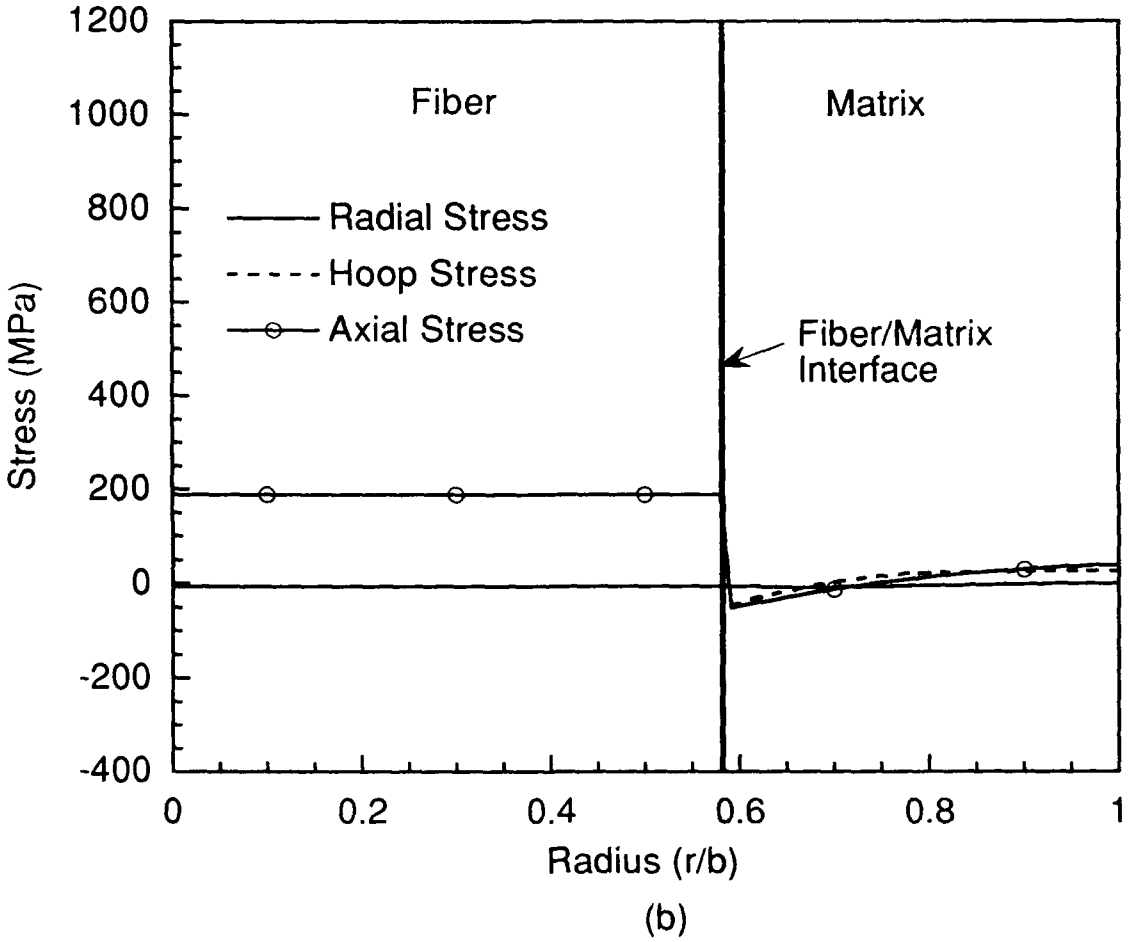

Figure 6.12b Variation of Predicted Stresses with Radius for an Out-of-Phase TMF Cycle at 650°C.

The axial stresses in the matrix at the fiber-matrix interface are shown in Fig. 6.13. The steps on the horizontal axis correspond to those of the TMF spectrum schematic in Fig. 6.11b. As noted in the discussion of the previous figure, the OOP cycle has tensile thermal stresses as well as tensile mechanical stresses at minimum temperature which corresponds to maximum load. This results in a large stress range in the matrix from approximately 450 MPa at minimum temperature (step 60) to approximately -50 MPa at maximum temperature (step 80). The IP cycle, on the other hand, has a much smaller stress range in the matrix material. At minimum temperature (step 60), there is a thermal residual stress but little contribution from applied (minimum) load. The net stress is approximately 275 MPa. When maximum temperature is reached (step 80), the thermal stress decreases and the mechanical stress increases. The net result is a stress decrease to approximately 200 MPa. In summary, the axial stress range in the matrix is large in an OOP cycle and small in an IP cycle.

In a similar fashion, the axial stress peaks in the fiber are compared for an IP and OOP TMF cycle in Fig. 6.14. In the fiber, the thermal stresses at low temperature are compressive because of the low value of a compared to that in the matrix. For an IP cycle, therefore, the axial stresses range from compressive, due to residual thermal stress at low temperature (step 60), to tension due to the applied maximum load at high temperature (step 80). In the OOP cycle, the compressive residual stress at low temperature is offset by the larger mechanical stress due to maximum load, resulting in a net tensile stress of approximately 1000 MPa at minimum temperature (step 60). Decreasing the load while increasing the temperature reduces the mechanical stress but also relaxes the compressive residual stress. Since the mechanical stress range exceeds the thermal stress range for this set of conditions, the net effect is a reduction in stress to approximately 200 MPa at maximum temperature (step 80). Thus, an in-phase cycle produces a larger stress range and higher maximum stress in the fiber than an out-of-phase cycle for the conditions evaluated here. This is in contrast to the stress range in the matrix which is maximum in the OOP cycle and smaller in the IP cycle.

The radial and hoop stresses in the matrix at the fiber-matrix interface are plotted in Fig. 6.15. Since the applied load is in the axial direction, its contribution to hoop and radial stresses is minimal and arises solely due to Poisson's ratio and 3-D plasticity effects. Thus, the stresses are mostly due to the thermal cycling, and the IP and OOP cycles produce a similar stress state. At minimum temperature (step 60), the hoop stresses in the matrix are

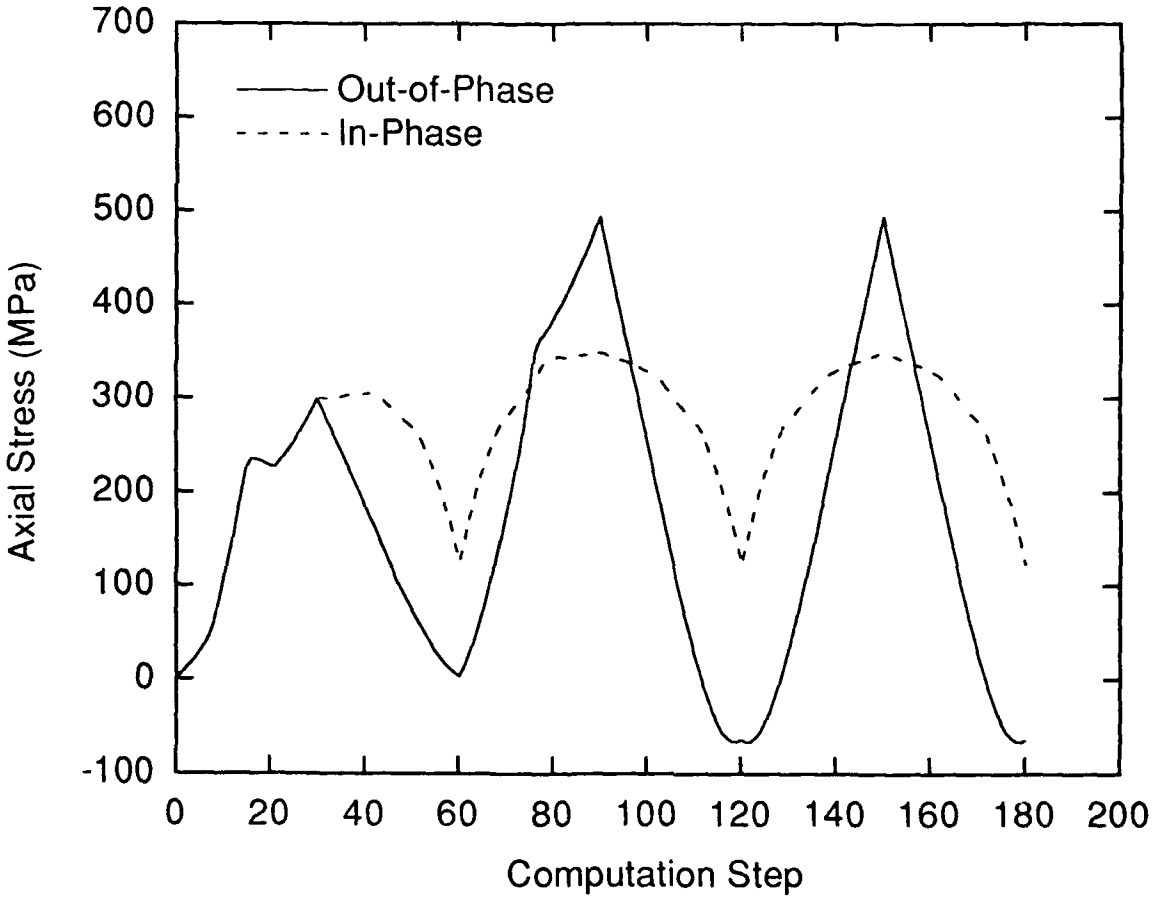

Figure 6.13 Axial Stress Predictions in the Ti-24Al-11Nb Matrix at the Fiber-Matrix Interface for In-Phase and Out-of-Phase TMF Cyclic Loading.

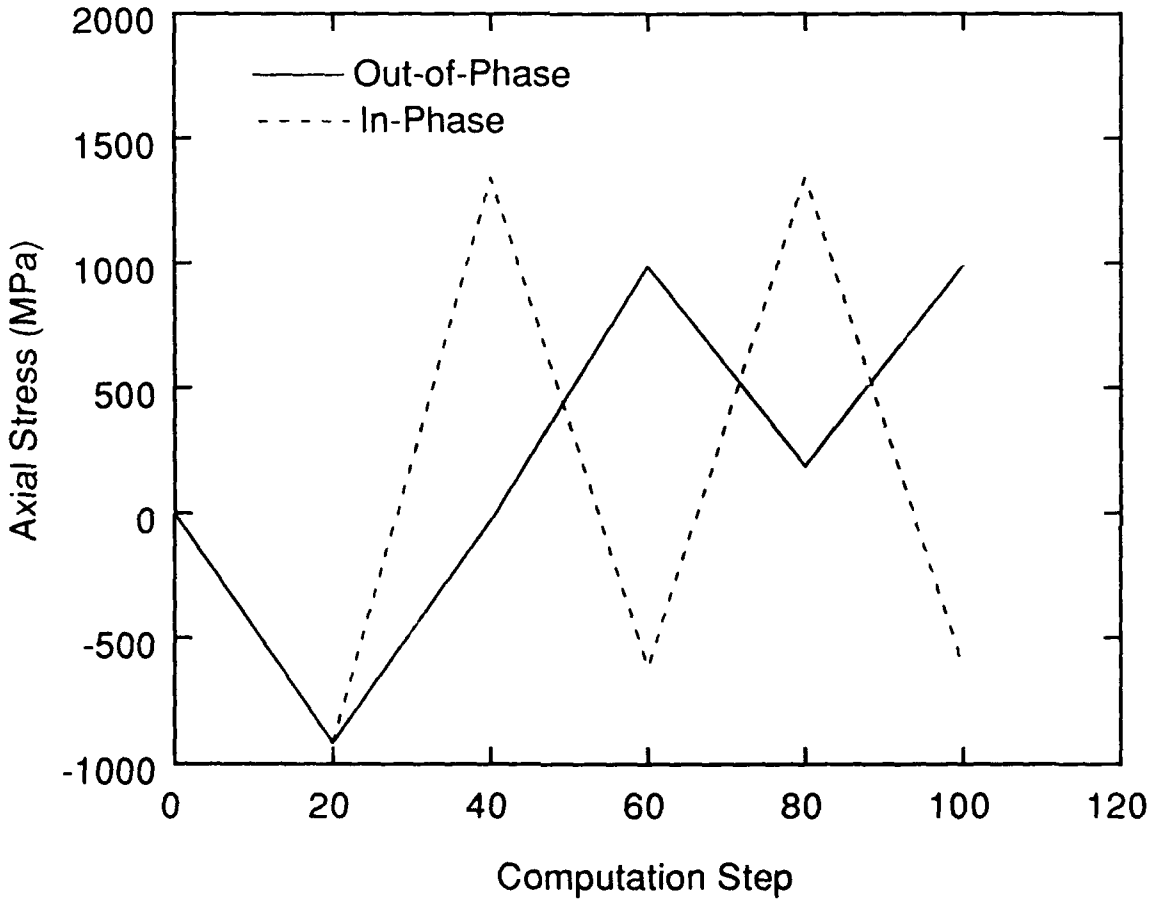

Figure 6.14 Axial Stress Peaks Predicted in the SCS-6 Fiber for In-Phase and Out-of-Phase TMF Cyclic Loading.

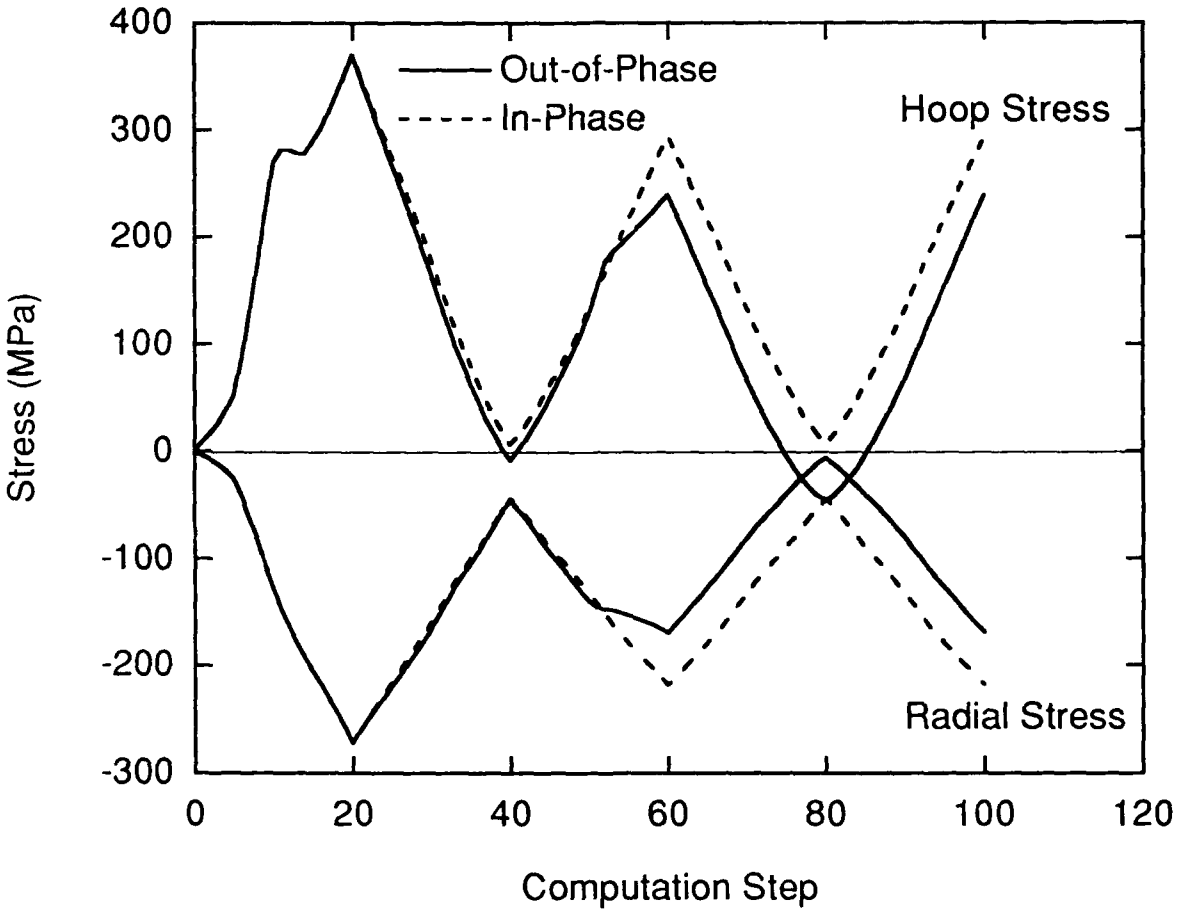

Figure 6.15 Radial and Hoop Stress Predictions in Ti-24Al-11Nb Matrix at the Fiber-Matrix Interface for In-Phase and Out-of-Phase TMF Cyclic Loading.

tensile whereas the radial stresses are compressive. At the maximum temperature (step 80), both components relax to nearly zero.

REFERENCES

[1] Foye, R. L., "Theoretical Post-Yielding Behavior of Composite Laminates, Part I - Inelastic Micromechanics", **Journal of Composites Materials**, Vol. 7, No. pp. 178-193, April 1973.

[2] Lin, T. H., Salinas, D., and Ito, Y. M., "Elastic-Plastic Analysis of Unidirectional Composites", **Journal of Composite Materials**, Vol. 6, No. pp. 48-60, 1972.

[3] Adams, D. F., "Inelastic Analysis of a Unidirectional Composite Subjected to Transverse Normal Loading", **Journal of Composite Materials**, Vol. 4, No. pp. 310-328, 1970.

[4] Foye, R. L., "Inelastic Micromechanics of Curing Stresses in Composites", **Inelastic Behavior of Composite Materials**, 1975 ASME Winter Annual Meeting, C. T. Herakovich, Eds., American Society of Mechanical Engineering, Houston, Texas, pp. 1975.

[5] Kolkailah, F. A. and McPhate, A. J., "Bodner-Partom Constitutive Model and Nonlinear Finite Element Analysis", **Journal of Engineering Materials and Technology**, Vol. 112, No. pp. 287-291, July 1990.

[6] Sherwood, J. A. and Boyle, M. J., "Investigation of the Thermomechanical Response of a Titanium-Aluminide/Silicon-Carbide Composite using a Unified State Variable Model and the Finite Element Method", **Microcracking-Induced Damage in Composites**, AMD-Vol. 111/MD-Vol. 22, , Eds., The American Society of Mechanical Engineers, pp. 151-161, 1990.

[7] Dvorak, G. J. and Bahei-El-Din, Y. A., "Plasticity Analysis of Fibrous Composites", **Journal of Applied Mechanics**, Vol. 49, No. pp. 327-335, June 1982.

[8] Bahei-El-Din, Y. A., **Plastic Analysis of Metal-Matrix Composite Laminates**, Ph. D. Dissertation, Duke University, 1979.

[9] Mirdamadi, M., Johnson, W. S., Bahei-El-Din, Y. A., and Castelli, M. G., **Analysis of Thermomechanical Fatigue of Unidirectional Titanium Metal Matrix Composites**, NASA Technical Memorandum 104105, July 1991.

[10] Aboudi, J., "Damage in Composites - Modeling of Imperfect Bonding", **Composites Science and Technology**, Vol. No. 28, pp. 103-128, 1987.

[11] Hopkins, D. A. and Chamis, C. C., "A Unique Set of Micromechanics Equations for High-Temperature Metal Matrix Composites", **Testing Technology of Metal Matrix Composites**, ASTM STP 964, P. R. DiGiovanni and N. R. Adsit, Eds., American Society for Testing and Materials, Philadelphia, pp. 159-176, 1988.

[12] Sun, C. T., Chen, J. L., Shah, G. T., and Koop, W. E., "Mechanical Characterization of SCS-6/Ti-6-4 Metal Matrix Composite", **Journal of Composite Materials**, Vol. 24, No. pp. 1029-1059, October 1990.

[13] Chamis, C. C. and Hopkins, D. A., "Thermoviscoplastic Nonlinear Consitutive Relationships for Structural Analysis of High-Temperature Metal Matrix Composites", **Testing Technology of Metal Matrix Composites**, ASTM STP 964, P. R. DiGiovanni and N. R. Adsit, Eds., American Society for Testing and Materials, Philadelphia, pp. 177-196, 1988.

[14] Chamis, C. C., Murthy, P. L. N., and Hopkins, D. A., "Computational Simulation of High-Temperature Metal Matrix Composites Cyclic Behavior", **Thermal and Mechanical Behavior of Metal Matrix and Ceramic Matrix Composites**, ASTM STP 1080, J. M. Kennedy, H. H. Moeller, andW. S. Johnson, Eds., American Society for Testing and Materials, Philadelphia. pp. 56-69, 1990.

[15] Bigelow, C. A., Johnson, W. S., and Naik, R. A., "A Comparison of Various Micromechanics Models for Metal Matrix Composites", **Mechanics of Composite Materials and Structures**, J. N. Reddy and J. L. Telpy, Eds., The American Society of Mechanical Engineers, Philadelphia, pp. 21-31, 1989.

[16] Mikata, Y. and Taya, M., "Stress Field in a Coated Continuous Fiber Composite Subjected to Thermo-Mechanical Loadings", **Journal of Composite Materials**, Vol. 19, No. pp. 554-578, November 1985.

[17] Vedula, M., Pangborn, R. N., and Queeney, R. A., "Modification of Residual Thermal Stress in a Metal-Matrix Composite with the use of a Tailored Interfacial Region", **Composites**, Vol. 19, No. 2, pp. 133-137, March 1988.

[18] Pagano, N. J. and Tandon, G. P., "Elastic Response of Multi-Directional Coated-Fiber Composites", **Composites Science and Technology**, Vol. 31, No. pp. 273-293, 1988.

[19] Ebert, L. J., Fedor, R. J., Hamilton, C. H., Hecker, S. S., and Wright, P. K., **Analytical Approach to Composite Behavior**, Technical Report AFML-TR-69-129, June 1969.

[20] Hecker, S. S., Hamilton, C. H., and Ebert, L. J., "Elastoplastic Analysis of Residual Stresses and Axial Loading in Composite Cylinders", **Journal of Materials, JMLSA**, Vol. 5, No. 4, pp. 868-900, December 1970.

[21] Gdoutos, E. E., Karalekas, D., and Daniel, I. M., "Thermal Stress Analysis of a Silicon Carbide/Aluminum Composite", **Experimental Mechanics**, Vol. 31, No. 3, pp. 202-208, September 1991.

[22] Gdoutos, E. E., Karalekas, D., and Daniel, I. M., "Micromechanical Analysis of Filamentary Metal Matrix Composites Under Longitudinal Loading", **Journal of Composites Technology and Research, JCTRER**, Vol. 13, No. 3, pp. 168-174, Fall 1991.

[23] Lee, J. W. and Allen, D. H., "An Analytical Solution for the Elastoplastic Response of a Continuous Fiber Composite Under Uniaxial Loading", **Research in Structures, Structural Dynamics and Materials 1990**, NASA Conference Publication 3064, pp. 55-65, 1990.

[24] Timoshenko, S. P. and Goodier, J. N., **Theory of Elasticity**, New York, McGraw-Hill Book Company, 1987.

[25] Mendelson, A., **Plasticity: Theory and Application**, New York, MacMillan, 1968.

[26] Chakrabarty, J., **Theory of Plasticity**, New York, McGraw-Hill Book Company, 1991.

[27] **IMSL FORTRAN Subroutines for Mathematical Applications, Math/Library Version 1.0**, IMSL, Houston, 1987.

[28] Ashbaugh, N. E., Khobaib, M., et al., **Mechanical Properties for Advanced Engine Materials**, WL-TR-91-4149, Materials Directorate, Wright Laboratory, Wright-Patterson AFB, Ohio, April 1992.

[29] Brockman, R. A., "MAGNA: A Finite System for Three Dimensional Nonlinear Static and Dynamic Structural Analysis", **Computers and Structures**, Vol. 13, No. pp. 415-423, 1981.

[30] Kroupa, J. L., "Elastic-Plastic Finite Element Analysis of MMC Subjected to Thermomechanical Fatigue", **Titanium Aluminide Composites, WL-TR-91-4020**, Wright Laboratory, Wright-Patterson AFB, Ohio, February, 1991.

APPENDIX A
LISTING OF FIDEP SOURCE CODE

```
      PROGRAM FIDEP3B
C  ************************************************************************
C
C     THIS PROGRAM COMPUTES ELASTIC-PLASTIC STRESSES IN AXISYMMETRIC
C     CONCENTRIC CYLINDERS SUBJECTED TO THERMOMECHANICAL CYCLIC
C     LOADING.
C
C     INPUT FILES:
C        FDMAT    TEMPERATURE DEPENDENT MATERIAL DATA
C        FDLOAD   THERMOMECHANICAL CYCLIC LOADING PROFILE
C     OUTPUT FILES:
C     AT INTERFACE:
C        FDOUTS   STRESSES AND AXIAL STRAIN AT EACH STEP
C        FDOUTE   STRAINS AT EACH STEP
C        FDSUM    STRESSES AND STRAINS CORRESPONDING TO FDLOAD
C     AT CROSS-SECTION:
C        FDUSP    STRESSES AND STRAINS AT THE END OF THE PROGRAM
C                 AT THE COMPOSITE CROSSSECTION
C
C     FINAL REVISION: 13-NOVEMBER-1991
C     PROGRAMMER: DEMIRKAN COKER (255-1361)
C     SUPERVISOR: NOEL E. ASHBAUGH
C                 UNIVERSITY OF DAYTON RESEARCH INSTITUTE
C
C  ************************************************************************
C     DEFINITION OF THE VARIABLES USED IN THE PROGRAM
C  /MAT1/
C  E(201)          MODULUS AT RADIUS R
C  VMU(201)        POISSON'S RATIO AT EACH R
C  CTE(201)        THERMAL EXPANSION COEFFICIENT AT EACH R
C  R(201)          RADIUS
C  VF              FIBER VOLUME FRACTION
C  EZ              EZ = EZSTAR - 2/EC*SR(INT+1)*VF*(VMU(INT)-VMU(INT+1))
C                  I.E. TOTAL AXIAL STRAIN = EZTOT
C  /MAT2/
C  EC              RULE OF MIXTURES COMPOSITE MODULUS
```

```
C  TEMP(5,20)      TEMPERATURES AT WHICH PROPERTIES ARE GIVEN FOR
C                  CONSTITUENTS
C  EMAT(5,20)      MODULI AT TEMPERATURE FOR THE CONSTITUENTS
C  CTEMAT(5,20)    CTES AT TEMPERATURE FOR THE CONSTITUENTS
C  VMUMAT(5,20)    POISSON'S RATIOS AT TEMPERATURE FOR THE CONSTITUENTS
C  /MAT3/
C  DT(200)         CURRENT TEMPERATURE MINUS REFERENCE TEMPERATURE
C  T(200)          CURRENT TEMPERATURE
C  ET(5,200)       CONSTITUENT MODULI INTERPOLATED FOR THE CURRENT
C                  TEMPERATURE
C  VMUT(5,200)     CONSTITUENT POISSON'S RATIIO "   "   "    "       "
C  CTET(5,200)     CONSTITUENT CTE INTERPOLATED    "   "    "       "
C  PZ(200)         APPLIED STRESS CORRESPONDING TO THE CURRENT STEP
C  /MAT4/
C  TINI,TFIN       INITIAL AND FINAL TEMPS READ FROM THE LOADING FILE
C  PINI,PFIN       INITIAL AND FINAL APPLIED STRESSES READ FROM THE
C                  LOADING FILE
C  TREF            REFERENCE TEMPERATURE FOR SECANT CTE = PROCESSING
C                  TEMPERATURE WHERE THE STRESSES ARE ASSUMED TO BE ZERO
C  /MAT5/
C  SYMAT(5,20)     ORIGINAL YIELD STRESS AT DEFINED TEMPERATURES
C  EPLMAT(5,20)    PLASTIC MODULUS FOR THE CONSTITUENTS AT DEFINED
C                  TEMPERATURES
C  /MAT6/
C  EPLT(5,200)     CONSTITUENT PLASTIC MODULI INTERPOLATED FOR THE
C                  CURRENT TEMP
C  SY(5,200)       CONSTITUENT ORIGINAL YIELD INTERPOLATED FOR THE
C                  CURRENT TEMP
C  /LIMITS/
C  NTOT            NUMBER OF NODES ALONG THE RADIUS MINUS 1 = NRA/2.
C  NRA             NUMBER OF ROWS OF MATRIX A
C  INT             NODE IN THE FIBER AT THE INTERFACE
C  /STRAINS/
C  ERTOT(201)      TOTAL RADIAL STRAIN
C  ETTOT(201)      TOTAL HOOP STRAIN
C  EZTOT(201)      TOTAL AXIAL STRAIN
```

```
C  /XX/
C  ERP(201),ETP(201),EZP(201)
C                 OLD PLASTIC STRAINS IN THE PLSTRAIN .NE. NEW PLASTIC
C                 STRAINS IN SUBROUTINE SOLVE WHICH DOES NOT USE THIS
C                 COMMON BLOCK
C  ERP2(201), ETP2(201), EZP2(201)
C                 PLASTIC STRAINS USED IN SUBROUTINES PLSTRAIN AND SOLVE
C  /LEG/
C  JAR            TO READ NRA FROM SUBROUTINE SOLVE AT THE BEGINNING
C  SR(201)        RADIAL STRESS ACROSS THE CROSSSECTION
C  ST(201)        HOOP STRESS ACROSS THE CROSS-SECTION
C  SZ(201)        AXIAL STRESS ACROSS THE CROSS-SECTION
C  NOMAT          NUMBER OF MATERIALS - FOR NOW 2
C  NROW(5)        NUMBER OF ROWS OF TEMPERATURE DEPENDENT DATA
C  SE(201)        CURRENT YIELD SURFACE - USED IN SUBROUTINE PLSTRAIN
C  TE(20)         TEMPERATURE READ FROM LOADING FILE
C  PAT(20)        APPLIED STRESS READ FROM LOADING FILE
C  NOT(20)        TOTAL NUMBER OF STEPS FOR EACH HALF CYCLE
C
C  ************************************************************************
      COMMON/MAT0/EF,EM,CTEF,CTEM
      COMMON/MAT1/EC,E(201),VMU(201),CTE(201),R(201),VF,EZ
      COMMON/MAT2/TEMP(5,20),EMAT(5,20),CTEMAT(5,20),VMUMAT(5,20)
      COMMON/MAT3/DT(200),T(200),ET(5,200),VMUT(5,200),CTET(5,200),PZ(200)
      COMMON/MAT4/TINI,TREF,TFIN,PINI,PFIN
      COMMON/MAT5/SYMAT(5,20), EPLMAT(5,20)
      COMMON/MAT6/EPLT(5,200), SY(5,200)
      COMMON/LIMITS/NTOT, NRA, INT
      COMMON/STRAINS/ERTOT(201), ETTOT(201), EZTOT(201)
      COMMON/LEG/JAR
      COMMON/EMECH/ETHERMAL,ERMECH,ETMECH,EZMECH
      REAL ERP2(201),ETP2(201),EZP2(201)
      REAL SR(201), ST(201), SZ(201), SEFF(201), SE(201)
      INTEGER NOMAT, NROW(5)
      INTEGER NTIME
      REAL TE(20), PAT(20), NOT(20)
```

```
      COMMON/WORKSP/RWKSP
      REAL RWKSP(100000)
      CALL IWKIN(100000)
      CALL UMACH(-2,12)

      OPEN(UNIT=11,FILE='FDMAT',STATUS='OLD')
      OPEN(UNIT=20,FILE='FDLOAD',STATUS='OLD')
      OPEN(UNIT=12, FILE='FDOUTS', STATUS='NEW')
      OPEN(UNIT=17, FILE='FDOUTE', STATUS='NEW')
      OPEN(UNIT=18, FILE='FDUSP', STATUS='NEW')
      OPEN(UNIT=19, FILE='FDSUM', STATUS='NEW')

      NTIME = 0

C - - - Start of timed sequence

      XT1=SECNDS(0.0)

C - - - Read dimension NRA of the matrix A to be solved

      JAR = 0
      CALL SOLVE(ILK,SR,ST,SZ,SEFF,B,ERP2,ETP2,EZP2)
      JAR = JAR + 1
      PRINT *, 'MATRIX DIMENSION IS', NRA

C - - - Read loading from input file FDLOAD.DAT

      READ(20,*)
      READ(20,*)                    !COMMENT LINES IN INPUT DATA
      READ(20,*)
      READ(20,*)
      READ(20,*) NLOAD
      READ(20,*) (NOT(I), I=1,NLOAD)
      READ(20,*) (TE(I), I=1,NLOAD)
      READ(20,*) (PAT(I), I=1,NLOAD)
```

```
      WRITE(12,*) 'NO OF DATA ', NLOAD
      WRITE(12,*) 'STEPS', (NOT(I), I=1,NLOAD)
      WRITE(12,*) 'TEMP ', (TE(I), I=1,NLOAD)
      WRITE(12,*) 'STRESS ', (PAT(I), I=1,NLOAD)
      TREF = TE(1)

C - - - Read temperature dependent material properties

      CALL READMAT(NOMAT,NROW)

C - - - Define nodes in the concentric cylinder model

      CALL GEOMETRY(VF,B,A,DR,R)

C - - - Print header lines

      CALL HEADER(NTIME,TE,PAT,NOT)

      CLOSE(11)
      CLOSE(20)

C - - - Start cyclic loading

      DO 995 ICYC = 1, NLOAD-1

         NSTEPS = NOT(ICYC+1)-NOT(ICYC)
         TINI = TE(ICYC)
         TFIN = TE(ICYC+1)
         PINI = PAT(ICYC)*1.0E6
         PFIN = PAT(ICYC+1)*1.0E6

         CALL LOADING(NSTEPS,NOMAT)

         DO 990 ILK=2,NSTEPS+1

             NTIME = NTIME + 1
```

```
C - - - Define properties at each node, i. e. translate properties at
C     temperature for material 1 and 2 into node properties; E,alpha,nu
C     In addition, define shorthands for moduli, Ef, Em, Ec.

            CALL PROPERTIES(ILK)

C - - - Calculate stresses with old  plastic strains (dep-new = 0)
C     i.e. assume loading increment to be elastic only

              CALL SOLVE(ILK,SR,ST,SZ,SEFF,B,ERP2,ETP2,EZP2)

C - - - Iterate to find plastic strain increments

              CALL PLSTRAIN(ILK,SR,ST,SZ,SEFF,B,ERP2,ETP2,EZP2,SE)

C - - - Output stresses and strains

              CALL OUTS(SEFF,SR,ST,SZ,ILK,NTIME,ERP2,ETP2,EZP2)

 990     CONTINUE

         CALL OUTSUM(INT,SZ,SR,ST,SEFF,NTIME,TFIN,PFIN)

 995  CONTINUE

C - - - Output stresses and strains at the cross-section

      CALL OUTUSP(SEFF,SR,ST,SZ,ERP2,ETP2,EZP2,NTOT)

C - - - Print out runtime of the code

      CALL REALTIME(NRA,NTIME,XT1)
 99   FORMAT(2X,I4,1X,F7.1,1X,F8.1,1X,5(F8.1,1X),E10.3)
      STOP
      END
```

```
C ------------------------------------------------------------------
C                              SUBROUTINES
C ------------------------------------------------------------------

C ------------------------------------------------------------------
C READ INPUT MATERIAL PROPERTIES FOR THE FIBER AND THE MATRIX
C ------------------------------------------------------------------

      SUBROUTINE READMAT(NOMAT,NROW)
      COMMON/MAT2/TEMP(5,20),EMAT(5,20),CTEMAT(5,20),VMUMAT(5,20)
      COMMON/MAT4/TINI,TREF,TFIN,PINI,PFIN
      COMMON/MAT5/SYMAT(5,20), EPLMAT(5,20)
      REAL TEMP,EMAT,CTEMAT,VMUMAT,TREF,TFIN,TREF2(5)
      INTEGER NOMAT,NROW(5)

C - - - Read temperature dependent material data

      READ(11,*)
      READ(11,*)
      READ(11,*)NOMAT
      DO 144 I=1,NOMAT
         READ(11,*) NROW(I)
         READ(11,*)
         DO 144 J=1,NROW(I)
            READ(11,*) TEMP(I,J),EMAT(I,J),CTEMAT(I,J),VMUMAT(I,J),
     +           SYMAT(I,J), EPLMAT(I,J)
            WRITE(12,99)I,J,TEMP(I,J),EMAT(I,J),CTEMAT(I,J),VMUMAT(I,J),
     +           SYMAT(I,J), EPLMAT(I,J)
144   CONTINUE
99    FORMAT(2(I5),2X,4(F8.2),E9.2,F8.2)
      READ(11,*)
      READ(11,*)TREF
      RETURN
      END
```

```
C ---------------------------------------------------------------------
C COMPUTE RADIUS OF NODES AND INTERFACE NODE IN THE CCM
C ---------------------------------------------------------------------

      SUBROUTINE GEOMETRY(VF,B,A,DR,R)
      COMMON/LIMITS/NTOT, NRA, INT
      REAL VF, B, A, DR, R(201)
      INTEGER NTOT, INT

      READ(11,*)
      READ(11,*,END=44) VF, B
      WRITE(12,*)'VF= ', VF
      GOTO 45
 44   VF = 0.35
      B = 1.
 45   A = SQRT(VF)/B
      PRINT *, 'VF, B ', VF, B
      NTOT = NRA/2.0
C - - - Nodes in Fiber
      R(1) = 0.02E-10
        R(2) = A/2
        R(3) = A - A/100.0
C - - - Nodes in Matrix
        R(4) = A + A/100.0
      DR = (B-A)/(NTOT-3)
      DO 10 I=5,NTOT+1
         R(I) = A + DR*(I-4)
 10   CONTINUE
      INT = 3                  ! A/DR + 1
        DO I=1,NTOT+1
          PRINT *, I, R(I)
        END DO
        PRINT *, ' rf, rm, A ', R(INT), R(INT+1),A
C     R(INT+1) = A
      RETURN
      END
```

```
C ------------------------------------------------------------------
C COMPUTE INCREMENTAL LOADING AND INTERMEDIATE PROPERTIES
C ------------------------------------------------------------------

      SUBROUTINE LOADING(NSTEPS,NOMAT)
      COMMON/MAT3/DT(200),T(200),ET(5,200),VMUT(5,200),CTET(5,200),PZ(200)
      COMMON/MAT4/TINI,TREF,TFIN,PINI,PFIN
      COMMON/MAT2/TEMP(5,20),EMAT(5,20),CTEMAT(5,20),VMUMAT(5,20)
      COMMON/MAT5/SYMAT(5,20), EPLMAT(5,20)
      COMMON/MAT6/EPLT(5,200), SY(5,200)

      DO 110 I=1,NSTEPS+1
         DTII = (I-1.)*(TFIN-TREF)/NSTEPS/1.
         DTEMP = (I-1.)*(TFIN-TINI)/NSTEPS/1.
         T(I) = TINI + DTEMP
         DPZ = (I-1.)*(PFIN-PINI)/NSTEPS/1.
         PZ(I) = PINI + DPZ
         DT(I) = T(I) - TREF
         TT = T(I)

C - - - Compute the material properties at each loading temperature

         DO K=1,NOMAT
            J=1
            DO WHILE(TT.GT.TEMP(K,J))
            J=J+1
            END DO
            TFACTOR=(TT-TEMP(K,J-1))/(TEMP(K,J)-TEMP(K,J-1))
            CALL INTERP(I,K,J,TFACTOR,ET,EMAT)
            CALL INTERP(I,K,J,TFACTOR,CTET,CTEMAT)
            CALL INTERP(I,K,J,TFACTOR,VMUT,VMUMAT)
            CALL INTERP(I,K,J,TFACTOR,SY,SYMAT)
            CALL INTERP(I,K,J,TFACTOR,EPLT,EPLMAT)
         END DO
```

```
 110  CONTINUE

      DO 120 K=1,NOMAT
        DO 120 I=1,NSTEPS+1
          SY(K,I) = SY(K,I)*1.E6
          EPLT(K,I) = EPLT(K,I)*1.E9
 120  CONTINUE
      RETURN
      END

C -----------------------------------------------------------------------
C INTERPOLATION SCHEME USED IN DETERMINING INTERMEDIATE PROPERTIES
C -----------------------------------------------------------------------

      SUBROUTINE INTERP(I,K,J,TFACTOR,VALT,VALMAT)
      REAL VALT(5,200), VALMAT(5,20), TFACTOR
      INTEGER I, K, J

      VALT(K,I)=VALMAT(K,J-1)+(VALMAT(K,J)-VALMAT(K,J-1))*TFACTOR

      RETURN
      END

C -----------------------------------------------------------------------
C ASSIGN PROPERTIES TO EACH NODE
C -----------------------------------------------------------------------

      SUBROUTINE PROPERTIES(ILK)
      COMMON/MAT0/EF,EM,CTEF,CTEM
      COMMON/MAT1/EC,E(201),VMU(201),CTE(201),R(201),VF,EZ
      COMMON/MAT3/DT(200),T(200),ET(5,200),VMUT(5,200),CTET(5,200),PZ(200)
      COMMON/MAT6/EPLT(5,200), SY(5,200)
      COMMON/LIMITS/NTOT, NRA, INT

      EF = ET(1,ILK)*1.E9                !414E9
      EM = ET(2,ILK)*1.E9                !113.7E9
```

```
      CTEF = CTET(1,ILK)*1.0E-6
      CTEM = CTET(2,ILK)*1.0E-6
      DO 21 I=1,INT
         E(I) = ET(1,ILK)*1.E9            !414.E9
         VMU(I) = VMUT(1,ILK)             !0.3
         CTE(I) = CTET(1,ILK)*1.E-6       !4.7E-6
21    CONTINUE
      DO 22 I=INT+1,NTOT+1
         E(I) = ET(2,ILK)*1.E9            !113.7E9
         VMU(I) = VMUT(2,ILK)             !0.22
         CTE(I) = CTET(2,ILK)*1.E-6       !9.44E-6
22    CONTINUE
      EC = EF*VF + EM*(1-VF)
      RETURN
      END
```

```
C ---------------------------------------------------------------------
C COMPUTE STRESSES GIVEN A PLASTIC STRAIN INCREMENT
C ---------------------------------------------------------------------

      SUBROUTINE SOLVE(ILK,SR,ST,SZ,SEFF,B,ERP,ETP,EZP)
      PARAMETER(NRA=100, LDA=NRA, IPATH=1)
      COMMON/LIMITS/NTOT,NNRA, INT
      COMMON/MAT0/EF,EM,CTEF,CTEM
      COMMON/MAT1/EC,E(201),VMU(201),CTE(201),R(201),VF,EZ
      COMMON/MAT3/DT(200),T(200),ET(5,200),VMUT(5,200),CTET(5,200),PZ(200)
      COMMON/MAT6/EPLT(5,200), SY(5,200)
      REAL ERP(201), ETP(201), EZP(201)
      COMMON/STRAINS/ERTOT(201), ETTOT(201), EZTOT(201)
      COMMON/LEG/JAR
      REAL AA(201), BB(201), CC(201), DD(201), FF(201), GG(201), HH(201)
      REAL QQ(201), PLAS(201), PP(201)
      REAL AMAT(NRA,NRA), BMAT(NRA), XSOL(NRA)
      REAL SR(201), ST(201), SZ(201), SEFF(201)

      NNRA = NRA
      IF (JAR.EQ.0)THEN
         RETURN
      END IF

C - - - Calculate Ez without the radial stress component at the interface

      TEGRAL = 0.
      DO I=INT+1,NTOT+1
       TEGRAL=TEGRAL+(R(I)-R(I-1))*(EZP(I)*R(I)+EZP(I-1)*R(I-1))/2
      END DO
      EZSTAR = PZ(ILK)/EC + DT(ILK)*
     +            (CTEF*EF*VF+CTEM*EM*(1-VF))/EC
      EZSTAR = EZSTAR + 2*TEGRAL*EM/B**2/EC

C - - - Compute coefficients for the FD equations to use in the A-matrix
```

```
      DO 30 I=2,NTOT+1
         AA(I) = (R(I)-R(I-1))/2/R(I)
         BB(I) = E(I)/E(I-1)
         CC(I) = R(I)/R(I-1)
         DD(I) = (1+VMU(I))*(VMU(I)+AA(I))
         FF(I) = (1+VMU(I))*(1-VMU(I)+AA(I))
         GG(I) = (1+VMU(I-1))*(VMU(I-1)-AA(I)*CC(I))*BB(I)
         HH(I) = (1+VMU(I-1))*(1-VMU(I-1)-AA(I)*CC(I))*BB(I)
         QQ(I) = E(I)*DT(ILK)*(CTE(I)*(1+VMU(I))-CTE(I-1)*(1+VMU(I-1)))
         PLAS(I) = AA(I)*(ERP(I)+CC(I)*ERP(I-1)) - ETP(I)*(1+AA(I))
     +           + ETP(I-1)*(1-AA(I)*CC(I)) + VMU(I)*(ERP(I)+ETP(I))
     +           - VMU(I-1)*(ERP(I-1)+ETP(I-1))
         PLAS(I) = E(I)*PLAS(I)
         PP(I) = PLAS(I) + E(I)*EZSTAR*(VMU(I)-VMU(I-1))
 30   CONTINUE

C - - - Initialize A and B

      DO 51 I=1,2*NTOT
         DO 52 J=1,2*NTOT
            AMAT(I,J)= 0.0
 52        CONTINUE
         BMAT(I) = 0.0
 51   CONTINUE

C - - - Construct the A-matrix and B-matrix

      AMAT(1,1) = AA(2)
      AMAT(NTOT+1,1) = (1 + VMU(1))*(1 - 2*VMU(1))*BB(2)
      DO 55 I=2,NTOT
         AMAT(I-1,I) = -1.0              ! upper left
         AMAT(I,I) = 1/CC(I+1)
         AMAT(NTOT+I-1,I) = DD(I)        ! lower left
         AMAT(NTOT+I,I)  = -GG(I+1)
         AMAT(I,NTOT+I-1) = AA(I+1)      ! upper right
         AMAT(NTOT+I,NTOT+I-1) = HH(I+1)  ! lower right
```

```
 55   CONTINUE

C - - - This is the vmu correction at the interface from the axial strain

      AMAT(NTOT+INT,INT) = 2*EM/EC*VF*(VMU(INT)-VMU(INT+1))**2 - GG(INT+1)

      DO 66 I=1,NTOT
         AMAT(I,NTOT+I) = AA(I+1)        ! upper right
         AMAT(NTOT+I,NTOT+I) = -FF(I+1)   ! lower right
         BMAT(I) = 0.
         BMAT(NTOT+I) = QQ(I+1) - PP(I+1)
 66   CONTINUE

C - - - Solve for the radial and hoop stresses

      CALL LSARG(NRA,AMAT,LDA,BMAT,IPATH,XSOL)

C - - - Enforce boundary conditions

      SR(NTOT+1) = 0.0
      ST(1) = XSOL(1)                 ! XSOL(1) = SR(1)

C - - - Extract radial and hoop stresses from XSOL

      DO 86 I=1,NTOT
         SR(I) = XSOL(I)
         ST(I+1) = XSOL(NTOT+I)
 86   CONTINUE

      EZ = EZSTAR - 2/E*SR(INT+1)*VF*(VMU(INT)-VMU(INT+1))

C - - - Compute axial and effective stresses

      DO 101 I=1,NTOT+1
         SZ(I) = E(I)*(EZ-EZP(I)) - CTE(I)*E(I)*DT(ILK)
     +          + VMU(I)*(SR(I)+ST(I))
```

```
          SQUARE = (SR(I)-ST(I))**2+(SR(I)-SZ(I))**2+(ST(I)-SZ(I))**2
          SEFF(I) = SQRT((SQUARE)/2.)
 101   CONTINUE

C - - - Compute total strains

      DO I=1,NTOT+1
      ERTOT(I)=(SR(I)-VMU(I)*(ST(I)+SZ(I)))/E(I)+CTE(I)*DT(ILK)+ERP(I)
      ETTOT(I)=(ST(I)-VMU(I)*(SR(I)+SZ(I)))/E(I)+CTE(I)*DT(ILK)+ETP(I)
      EZTOT(I)=(SZ(I)-VMU(I)*(ST(I)+SR(I)))/E(I)+CTE(I)*DT(ILK)+EZP(I)
      END DO

      RETURN
      END

C ---------------------------------------------------------------------
C SUBROUTINE TO COMPUTE PLASTIC STRAIN INCREMENTS USING MENDELSON'S
C ALGORITHM
C ---------------------------------------------------------------------

      SUBROUTINE PLSTRAIN(ILK,SR,ST,SZ,SEFF,B,ERP2,ETP2,EZP2,SE)
      COMMON/LIMITS/NTOT,NNRA, INT
      COMMON/MAT0/EF,EM,CTEF,CTEM
      COMMON/MAT1/EC,E(201),VMU(201),CTE(201),R(201),VF,EZ
      COMMON/MAT3/DT(200),T(200),ET(5,200),VMUT(5,200),CTET(5,200),PZ(200)
      COMMON/MAT6/EPLT(5,200), SY(5,200)
      COMMON/LEG/JAR
      COMMON/STRAINS/ERTOT(201), ETTOT(201), EZTOT(201)
      COMMON/XX/ERP(201), ETP(201), EZP(201)
      COMMON/XXFEB6/DRTEST1(201), DRTEST2(201), DRTEST3(201)
      COMMON/XXFEB6/DTTEST1(201), DTTEST2(201), DTTEST3(201),EPEFF(201)
      REAL SR(201), ST(201), SZ(201), SEFF(201)
      REAL SE(201)
      REAL DERP(201), DETP(201), DEZP(201), DEP(201)
      REAL ERP2(201), ETP2(201), EZP2(201)
      REAL ERPCHECK(201), ETPCHECK(201)
```

```
      REAL YLDFLG(201)
      REAL DELTAR1(201),DELTAR2(201)
      REAL DELTAT1(201),DELTAT2(201)
      REAL ARCOEF(201),BRCOEF(201),ATCOEF(201),BTCOEF(201)
      INTEGER K, J, JJJ

C     DT: Current temperature minus the reference temperature

      ITER = 0
      IZMIR = 0

C - - - Calculate new yield surface after strain-hardening

      DO I = INT+1, NTOT+1
          XM = EPLT(2,ILK)/E(I)
          DSDE = XM*E(I)/(1.-XM)
          SE(I) = DSDE*EPEFF(I) + SY(2,ILK)
      END DO

C - - - Check if the new stresses are greater than new Y.S.

 8    DO I = INT+1, NTOT+1
         IF(SEFF(I).GT.SE(I)) GO TO 9
      END DO
      RETURN

C - - - If there is yielding of some nodes, start iterating for dep

 9    DO 55 KZ=1,12
           DO 10 I = INT+1, NTOT+1

C - - - Calculate new yield surface due to plas strain incr. at node i

             XM = EPLT(2,ILK)/E(I)
             DSDE = XM*E(I)/(1.-XM)
             SE(I) = DSDE*EPEFF(I) + SY(2,ILK)
```

```
            F = SEFF(I) - SE(I)

C - - - Check stress state for yielding at node i

            IF(F.GT.0) GOTO 50
            YLDFLG(I) = 0.
            GOTO 10
 50         YLDFLG(I) = 2.0

C - - - Calculate modified total strains

            ERMTS = ERTOT(I) - ERP(I)    ! erp is w/o derp
            ETMTS = ETTOT(I) - ETP(I)    ! W/O DETP(I)
            EZP(I) = -ERP(I) - ETP(I)
            EZMTS = EZTOT(I) - EZP(I)    ! W/O DEZP(I)
            SS1 = ERMTS - ETMTS
            SS2 = EZMTS - ETMTS
            SS3 = ERMTS - EZMTS

C - - - Calculate equivalent (effective) modified total strain (MTS)

            EET = SQRT(SS1**2+SS2**2+SS3**2)*SQRT(2.)/3.

C - - - Relationship between dep or PSI and eff MTS

            DENOMDEP = 1. + 2./3.*(1+VMU(I))/E(I)*DSDE
            DEP(I) = EET - 2./3.*(1+VMU(I))/E(I)*SE(I)
            DEP(I) = DEP(I)/DENOMDEP

C - - - Calculate new PSIs using modified Prandtl-Reuss equations

            DERP(I) = DEP(I)/3./EET*(2*ERMTS-ETMTS-EZMTS)
            DETP(I) = DEP(I)/3./EET*(2*ETMTS-ERMTS-EZMTS)
            DEZ2 = DEP(I)/3./EET*(2*EZMTS-ETMTS-ERMTS)
            DEZP(I) = -(DERP(I) + DETP(I))     ! Compare dezp & dez2
            ERP2(I) = ERP(I) + DERP(I)
```

```
              ETP2(I) = ETP(I) + DETP(I)
              EZP2(I) = -ERP2(I) - ETP2(I)
              EZP2TEST = EZP(I) + DEZP(I)
 10         CONTINUE

C - - -      Solve O.D.E.s with new plastic strain increments

 11         CALL SOLVE(ILK,SR,ST,SZ,SEFF,B,ERP2,ETP2,EZP2)

C - - - Save old plastic strains from the three previous iterations

            DO I = INT+1, NTOT+1
             DRTEST1(I) = DRTEST2(I)
               DRTEST2(I) = DRTEST3(I)
               DRTEST3(I) = ERP2(I)
               DTTEST1(I) = DTTEST2(I)
               DTTEST2(I) = DTTEST3(I)
               DTTEST3(I) = ETP2(I)
            END DO

C - - - Faster convergence scheme extrapolates the difference between
C     previous plastic strain increments to zero.

            IZMIR = IZMIR + 1
            IF(IZMIR.EQ.4)THEN
            IZMIR = 0
            DO 22 I = INT+1, NTOT+1
             PRODTEST = DRTEST1(I)*DRTEST2(I)*DRTEST3(I)
             DRDRTEST = ABS(DRTEST2(I)-DRTEST3(I))
             DTDTTEST = ABS(DTTEST2(I)-DTTEST3(I))
             IF(PRODTEST.NE.0.000000.AND.DRDRTEST.GT.1E-8.AND.
     +            DTDTTEST.GT.1.E-10)THEN
               DELTAR1(I) = DRTEST2(I) - DRTEST1(I)
               DELTAR2(I) = DRTEST3(I) - DRTEST2(I)
               ARCOEF(I) = (DELTAR1(I)-DELTAR2(I))/(DRTEST2(I)-DRTEST3(I))
               BRCOEF(I) = DELTAR2(I) -ARCOEF(I)*DRTEST3(I)
```

```
            if(atcoef(i).gt.1e-14)then
              ERP2(I) = - BRCOEF(I)/ARCOEF(I)
            end if
            DELTAT1(I) = DTTEST2(I) - DTTEST1(I)
            DELTAT2(I) = DTTEST3(I) - DTTEST2(I)
            ATCOEF(I) = (DELTAT1(I)-DELTAT2(I))/(DTTEST2(I)-DTTEST3(I))
            BTCOEF(I) = DELTAT2(I) -ATCOEF(I)*DTTEST3(I)
            if(atcoef(i).gt.1e-14)then
              ETP2(I) = - BTCOEF(I)/ATCOEF(I)
            end if
            EZP2(I) = - ERP2(I) - ETP2(I)
          END IF
22        CONTINUE
          GOTO 11
        END IF
55    CONTINUE

      DO M = INT+1, NTOT+1
        ERP(M) = ERP2(M)
        ETP(M) = ETP2(M)
        EZP(M) = -ERP(M) -ETP(M)
        EPEFF(M) = EPEFF(M) + DEP(M)
      END DO
      RETURN
      END
```

```
C ---------------------------------------------------------------------
C HEADER LINES FOR THE OUTPUT
C ---------------------------------------------------------------------

      SUBROUTINE HEADER(NTIME,TE,PAT,NOT)
      REAL TE(20), PAT(20), NOT(20)

      WRITE(12,750)
      WRITE(19,751)
      WRITE(17,752)
      WRITE(18,753)
 750    FORMAT(1X,'STEP ','TEMP ','APPSTRESS ','SEFF ',' SR ',' ST ',
     $         ' SZ ',' SY(MPA) ', 'EZMECH')
 751    FORMAT(1X,'STEP ','TEMP ','APPSTRESS ','SZF ',' SZM ',' SEFFM ',
     $         ' EEFFM ',' EZMECH ')
 752    FORMAT(1X,'STEP ','TEMP ','ERPM ','ETPM ',' EZPM ',' ERMECH ',
     $         ' ETMECH ',' EZMECH ', 'ETHERMAL')
 753    FORMAT(1X,'R/B ','SEFF ',' SR ',' ST ',
     $         ' SZ ',' ERP ', 'ETP ', 'EZP')
      RETURN
      END

C ---------------------------------------------------------------------
C PRINT STRESS OUTPUT IN FDOUTS.DAT AND STRAIN OUTPUT IN FDOUTE.DAT
C ---------------------------------------------------------------------

      SUBROUTINE OUTS(SEFF,SR,ST,SZ,ILK,NTIME,ERP2,ETP2,EZP2)
      COMMON/MAT0/EF,EM,CTEF,CTEM
      COMMON/MAT1/EC,E(201),VMU(201),CTE(201),R(201),VF,EZ
      COMMON/MAT3/DT(200),T(200),ET(5,200),VMUT(5,200),CTET(5,200),PZ(200)

      COMMON/MAT6/EPLT(5,200), SY(5,200)
      COMMON/LIMITS/NTOT, NRA, INT
      COMMON/STRAINS/ERTOT(201), ETTOT(201), EZTOT(201)
      COMMON/EMECH/ETHERMAL,ERMECH,ETMECH,EZMECH
      REAL ERP2(201),ETP2(201),EZP2(201)
```

```
      REAL SR(201), ST(201), SZ(201), SEFF(201)

      ICYC = ICYC + 1

      IF(ICYC.EQ.1)THEN
         WRITE(12,99) NTIME, TE(1), PAT(1)/1.E6, SEFF(1)/1.E6,
     +   SR(1)/1.E6, ST(1)/1.E6, SZ(1)/1.E6, SY(2,1)/1.E6,EZMECH
      END IF

      SS1 = SEFF(INT+1)/1.E6
      SS2 = SR(INT+1)/1.E6
      SS3 = ST(INT+1)/1.E6
      SS4 = SZ(INT+1)/1.E6
      SS5 = SY(2,ILK)/1.E6
      ETHERMAL = CTE(INT+1)*DT(ILK)
      ERMECH = ERTOT(INT+1) - ETHERMAL
      ETMECH = ETTOT(INT+1) - ETHERMAL
      EZMECH = EZTOT(INT+1) - ETHERMAL
      WRITE(12,99) NTIME, T(ILK), PZ(ILK)/1.E6, SS1, SS2, SS3, SS4,
     +     SS5, EZMECH
        L = INT+1
      WRITE(17,101)  NTIME, T(ILK), ERP2(L), ETP2(L), EZP2(L)
     +         , ERMECH, ETMECH, EZMECH, ETHERMAL
99    FORMAT(2X,I4,1X,F7.1,1X,F8.1,1X,5(F8.1,1X),E10.3)
101   FORMAT(2X,I5,2X,F7.2,7(2X,E11.5))
      RETURN
      END
```

```
C ------------------------------------------------------------------
C PRINT SUMMARIZED OUTPUT IN FDSUM.DAT
C ------------------------------------------------------------------

      SUBROUTINE OUTSUM(INT,SZ,SR,ST,SEFF,NTIME,TFIN,PFIN)
      COMMON/STRAINS/ERTOT(201), ETTOT(201), EZTOT(201)
      COMMON/EMECH/ETHERMAL,ERMECH,ETMECH,EZMECH
      REAL SR(201), ST(201), SZ(201), SEFF(201)

      XSZF = SZ(INT)/1.E6
      XSZM = SZ(INT+1)/1.E6
      XSEFFM = SEFF(INT+1)/1.E6
      IZ = INT+1
      SQUARE = (ERTOT(IZ)-ETTOT(IZ))**2 + (ERTOT(IZ)-EZTOT(IZ))**2 +
     +                 (ETTOT(IZ)-EZTOT(IZ))**2
      XEEFFM = SQRT((SQUARE)*2.)/3.
      XEMECH = EZTOT(INT+1) - ETHERMAL
      WRITE(19,222) NTIME, TFIN, PFIN/1.E6,
     +                    XSZF, XSZM, XSEFFM, XEEFFM, XEMECH
 222  FORMAT(I6,2(1X,F9.2),3(1X,F9.2),2(1X,E12.4))
      RETURN
      END

C ------------------------------------------------------------------
C PRINT OUTPUT AT THE CROSS-SECTION IN FDUSP.DAT
C ------------------------------------------------------------------

      SUBROUTINE OUTUSP(SEFF,SR,ST,SZ,ERP2,ETP2,EZP2,NTOT)
      COMMON/MAT0/EF,EM,CTEF,CTEM
      COMMON/MAT1/EC,E(201),VMU(201),CTE(201),R(201),VF,EZ
      REAL ERP2(201),ETP2(201),EZP2(201)
      REAL SR(201), ST(201), SZ(201), SEFF(201)

      DO I=1,NTOT+1
         SS1 = SEFF(I)/1.E6
         SS2 = SR(I)/1.E6
```

```
         SS3 = ST(I)/1.E6
         SS4 = SZ(I)/1.E6
       WRITE(18,88) R(I),SS1,SS2,SS3,SS4,ERP2(I),ETP2(I),EZP2(I)
       END DO
88     FORMAT(2X,F7.4,2X,4(F9.2,1X),3(F9.5,1X))
       RETURN
       END

C ---------------------------------------------------------------------
C COMPUTE RUNTIME
C ---------------------------------------------------------------------

       SUBROUTINE REALTIME(NRA,NTIME,XT1)
       DELTA = SECNDS(XT1)/60.
       WRITE(12,*) 'RUNTIME IS ',DELTA,' MIN FOR ', NRA,' NODES ',
      $      NTIME, 'TIME INCRS.'
       PRINT *, 'RUNTIME IS ',DELTA,' MIN FOR ', NRA,' NODES ',
      $      NTIME, 'TIME INCRS.'
       RETURN
       END
```

APPENDIX B
ELASTIC SOLUTION OF TWO CONCENTRIC CYLINDERS

Stresses in the matrix and the fiber are given by [28];

$$\sigma_{rm} = A(1-\frac{b^2}{r^2}) + P_r \frac{b^2}{r^2}, \qquad \sigma_{rf} = A(1-\frac{b^2}{a^2}) + P_r \frac{b^2}{a^2},$$

$$\sigma_{\theta m} = A(1+\frac{b^2}{r^2}) - P_r \frac{b^2}{r^2}, \qquad \sigma_{\theta f} = \sigma_{rf},$$

$$\sigma_{zm} = C, \qquad \sigma_{zf} = C(1-\frac{b^2}{a^2}) + P_z \frac{b^2}{a^2},$$

where;

$$A = \frac{s_2}{t_2 s_1 - t_1 s_2}\left(\frac{b^2}{a^2}(u_1 - u_2 \frac{s_1}{s_2}) + (\alpha_m - \alpha_f)T\right)$$

$$C = \frac{t_2}{t_2 s_1 - t_1 s_2}\left(\frac{b^2}{a^2}(u_1 - u_2 \frac{t_1}{t_2}) + (\alpha_m - \alpha_f)T\right)$$

$$s_1 = (1-\frac{b^2}{a^2})\frac{1}{E_f} - \frac{1}{E_m},$$

$$s_2 = (1-\frac{b^2}{a^2})\frac{(1+\nu_f)}{E_f} - \frac{(1+\nu_m)}{E_m},$$

$$t_1 = (1-\frac{b^2}{a^2})\frac{2\nu_f}{E_f} - \frac{2\nu_m}{E_m},$$

$$t_2 = (1-\frac{b^2}{a^2})\frac{(1+\nu_f)}{E_f} - (1+\frac{b^2}{a^2})\frac{(1+\nu_m)}{E_m},$$

$$u_1 = P_r \frac{2\nu_f}{E_f} - \frac{P_z}{E_m},$$

$$u_2 = (P_r - P_z)\frac{(1+\nu_f)}{E_f} - P_r \frac{(1+\nu_m)}{E_m}.$$

APPENDIX C
SAMPLE OUTPUT FILES

FDOUTS.DAT

NO OF DATA 2

STEPS		0.0000000E+00		30.00000				
TEMP		1010.000		20.00000				
STRESS		0.0000000E+00		0.0000000E+00				
1	1	20.00	414.00	4.70	0.22	0.10E+10	0.00	
1	2	93.00	414.00	4.81	0.22	0.10E+10	0.00	
1	3	204.00	414.00	4.97	0.22	0.10E+10	0.00	
1	4	316.00	414.00	5.12	0.22	0.10E+10	0.00	
1	5	427.00	414.00	5.26	0.22	0.10E+10	0.00	
1	6	538.00	414.00	5.38	0.22	0.10E+10	0.00	
1	7	649.00	414.00	5.50	0.22	0.10E+10	0.00	
1	8	760.00	414.00	5.60	0.22	0.10E+10	0.00	
1	9	871.00	414.00	5.70	0.22	0.10E+10	0.00	
1	10	982.00	414.00	5.78	0.22	0.10E+10	0.00	
1	11	1010.00	414.00	5.80	0.22	0.10E+10	0.00	
2	1	20.00	94.00	12.33	0.30	0.60E+03	1.30	
2	2	93.00	92.00	12.47	0.30	0.56E+03	0.90	
2	3	204.00	91.00	12.78	0.30	0.50E+03	0.72	
2	4	316.00	89.00	13.21	0.30	0.45E+03	0.69	
2	5	427.00	79.00	13.75	0.30	0.42E+03	0.41	
2	6	538.00	70.00	14.42	0.30	0.38E+03	0.11	
2	7	649.00	49.50	15.20	0.30	0.36E+03	0.00	
2	8	760.00	24.50	16.09	0.30	0.25E+03	2.35	
2	9	871.00	18.00	17.11	0.30	0.14E+03	2.63	
2	10	982.00	15.90	18.25	0.30	0.38E+02	1.18	
2	11	1010.00	15.00	18.55	0.30	0.30E+02	1.00	

VF = 0.3500000

STEP	TEMP	APPSTRESS	SEFF	SR	ST	SZ	SY(MPA)	EZMECH
0	1010.0	0.0	0.0	0.0	0.0	0.0	30.0	0.000E+00
1	977.0	0.0	11.0	-3.6	7.5	7.3	42.6	0.381E-03
2	944.0	0.0	22.2	-7.2	15.2	14.7	72.4	0.741E-03
3	911.0	0.0	33.6	-10.9	23.1	22.3	102.2	0.108E-02
4	878.0	0.0	45.2	-14.7	31.1	29.9	132.0	0.140E-02
5	845.0	0.0	60.0	-19.6	41.3	39.6	165.0	0.169E-02
6	812.0	0.0	76.9	-25.1	53.0	50.5	198.9	0.196E-02
7	779.0	0.0	95.1	-31.1	65.6	62.2	232.9	0.222E-02
8	746.0	0.0	124.4	-40.8	86.2	80.7	265.5	0.243E-02

9	713.0	0.0	171.3	-56.6	119.4	109.6	296.5	0.259E-02
10	680.0	0.0	222.6	-73.9	156.0	140.5	327.4	0.273E-02
11	647.0	0.0	277.1	-92.5	195.2	172.7	356.9	0.284E-02
12	614.0	0.0	329.3	-110.3	232.9	203.0	364.2	0.297E-02
13	581.0	0.0	371.5	-128.9	259.5	223.1	371.5	0.308E-02
14	548.0	0.0	378.9	-145.0	251.4	213.6	378.8	0.318E-02
15	515.0	0.0	389.6	-156.2	251.6	212.2	389.3	0.331E-02
16	482.0	0.0	401.8	-165.7	255.1	213.3	401.2	0.345E-02
17	449.0	0.0	414.0	-174.6	259.2	216.2	413.1	0.357E-02
18	416.0	0.0	424.9	-183.0	262.5	217.8	423.6	0.370E-02
19	383.0	0.0	433.1	-190.3	263.9	218.0	431.3	0.383E-02
20	350.0	0.0	441.4	-197.0	266.1	219.0	439.0	0.396E-02
21	317.0	0.0	449.8	-203.0	269.0	220.8	446.8	0.409E-02
22	284.0	0.0	464.8	-210.2	277.5	227.8	461.6	0.424E-02
23	251.0	0.0	480.0	-217.4	286.2	234.9	476.6	0.438E-02
24	218.0	0.0	495.2	-224.6	295.0	242.0	491.6	0.452E-02
25	185.0	0.0	512.5	-232.5	305.3	250.2	508.6	0.467E-02
26	152.0	0.0	531.4	-241.1	316.6	259.3	527.0	0.483E-02
27	119.0	0.0	550.2	-249.7	327.9	268.3	545.5	0.498E-02
28	86.0	0.0	569.6	-258.5	339.6	277.6	564.2	0.513E-02
29	53.0	0.0	590.8	-268.3	352.3	287.5	584.1	0.530E-02
30	20.0	0.0	612.1	-278.0	365.0	297.5	604.0	0.546E-02

RUNTIME IS 4.691536 MIN FOR 100 NODES 30 TIME INCRS.

FDOUTE.DAT

STEP	TEMP	ERPM	ETPM	EZPM	ERMECH	ETMECH	EZMECH	ETHERMAL
1	977.00	0.00000E+00	0.00000E+00	0.00000E+00	-.50091E-03	0.40110E-03	0.38106E-03	-.60043E-03
2	944.00	0.00000E+00	0.00000E+00	0.00000E+00	-.97558E-03	0.78203E-03	0.74094E-03	-.11786E-02
3	911.00	0.00000E+00	0.00000E+00	0.00000E+00	-.14241E-02	0.11428E-02	0.10798E-02	-.17345E-02
4	878.00	0.00000E+00	0.00000E+00	0.00000E+00	-.18465E-02	0.14834E-02	0.13978E-02	-.22682E-02
5	845.00	0.00000E+00	0.00000E+00	0.00000E+00	-.22450E-02	0.18087E-02	0.16921E-02	-.27842E-02
6	812.00	0.00000E+00	0.00000E+00	0.00000E+00	-.26193E-02	0.21172E-02	0.19644E-02	-.32811E-02
7	779.00	0.00000E+00	0.00000E+00	0.00000E+00	-.29695E-02	0.24079E-02	0.22159E-02	-.37582E-02
8	746.00	0.00000E+00	0.00000E+00	0.00000E+00	-.32879E-02	0.26848E-02	0.24269E-02	-.42191E-02
9	713.00	0.00000E+00	0.00000E+00	0.00000E+00	-.35712E-02	0.29501E-02	0.25875E-02	-.46672E-02
10	680.00	0.00000E+00	0.00000E+00	0.00000E+00	-.38304E-02	0.31991E-02	0.27255E-02	-.50975E-02
11	647.00	0.00000E+00	0.00000E+00	0.00000E+00	-.40679E-02	0.34325E-02	0.28443E-02	-.55110E-02
12	614.00	0.00000E+00	0.00000E+00	0.00000E+00	-.43076E-02	0.36644E-02	0.29696E-02	-.59202E-02
13	581.00	-.27147E-03	0.15574E-03	0.11573E-03	-.46813E-02	0.38815E-02	0.30797E-02	-.63141E-02
14	548.00	-.12155E-02	0.69870E-03	0.51684E-03	-.53897E-02	0.40858E-02	0.31827E-02	-.66927E-02
15	515.00	-.17844E-02	0.10265E-02	0.75790E-03	-.58941E-02	0.42944E-02	0.33118E-02	-.70679E-02
16	482.00	-.22078E-02	0.12709E-02	0.93689E-03	-.63180E-02	0.44990E-02	0.34468E-02	-.74350E-02
17	449.00	-.26011E-02	0.14983E-02	0.11028E-02	-.67096E-02	0.46938E-02	0.35738E-02	-.77892E-02
18	416.00	-.30096E-02	0.17350E-02	0.12747E-02	-.70986E-02	0.48865E-02	0.36992E-02	-.81373E-02
19	383.00	-.34759E-02	0.20054E-02	0.14706E-02	-.75130E-02	0.50867E-02	0.38322E-02	-.84879E-02
20	350.00	-.39144E-02	0.22598E-02	0.16546E-02	-.79002E-02	0.52795E-02	0.39618E-02	-.88279E-02
21	317.00	-.43274E-02	0.24997E-02	0.18278E-02	-.82628E-02	0.54647E-02	0.40885E-02	-.91572E-02
22	284.00	-.45468E-02	0.26270E-02	0.19198E-02	-.85854E-02	0.56661E-02	0.42370E-02	-.95005E-02
23	251.00	-.47521E-02	0.27463E-02	0.20059E-02	-.88971E-02	0.58629E-02	0.43817E-02	-.98362E-02
24	218.00	-.49490E-02	0.28606E-02	0.20884E-02	-.91988E-02	0.60542E-02	0.45217E-02	-.10164E-01
25	185.00	-.51327E-02	0.29673E-02	0.21654E-02	-.95111E-02	0.62578E-02	0.46703E-02	-.10499E-01
26	152.00	-.53078E-02	0.30691E-02	0.22387E-02	-.98325E-02	0.64708E-02	0.48256E-02	-.10841E-01
27	119.00	-.54784E-02	0.31683E-02	0.23101E-02	-.10149E-01	0.66810E-02	0.49783E-02	-.11177E-01
28	86.00	-.56582E-02	0.32730E-02	0.23852E-02	-.10470E-01	0.68942E-02	0.51322E-02	-.11512E-01
29	53.00	-.58875E-02	0.34065E-02	0.24809E-02	-.10831E-01	0.71282E-02	0.52986E-02	-.11863E-01
30	20.00	-.61171E-02	0.35404E-02	0.25767E-02	-.11189E-01	0.73614E-02	0.54640E-02	-.12213E-01

FDUSP.DAT

R/B	SEFF	SR	ST	SZ	ERP	ETP	EZP
0.0000	706.25	-284.48	-284.48	-990.73	0.00000	0.00000	0.00000
0.2958	706.25	-284.48	-284.48	-990.73	0.00000	0.00000	0.00000
0.5857	706.25	-284.48	-284.48	-990.73	0.00000	0.00000	0.00000
0.5975	612.10	-278.05	365.01	297.49	-0.00612	0.00354	0.00258
0.6003	611.95	-275.07	366.82	301.72	-0.00601	0.00346	0.00255
0.6090	611.49	-265.87	372.35	314.81	-0.00567	0.00321	0.00245
0.6177	611.06	-256.86	377.63	327.70	-0.00534	0.00298	0.00236
0.6264	610.64	-248.02	382.66	340.38	-0.00503	0.00276	0.00227
0.6351	610.25	-239.36	387.44	352.87	-0.00474	0.00255	0.00218
0.6437	609.87	-230.87	391.96	365.15	-0.00445	0.00236	0.00209
0.6524	609.51	-222.55	396.24	377.24	-0.00418	0.00217	0.00201
0.6611	609.17	-214.39	400.28	389.13	-0.00392	0.00200	0.00192
0.6698	608.84	-206.39	404.07	400.81	-0.00367	0.00184	0.00183
0.6785	608.52	-198.55	407.62	412.30	-0.00343	0.00168	0.00175
0.6872	608.22	-190.86	410.93	423.59	-0.00320	0.00154	0.00166
0.6959	607.93	-183.33	414.00	434.68	-0.00298	0.00141	0.00158
0.7046	607.66	-175.94	416.84	445.57	-0.00277	0.00128	0.00149
0.7133	607.40	-168.71	419.44	456.26	-0.00257	0.00116	0.00141
0.7219	607.14	-161.61	421.82	466.74	-0.00238	0.00105	0.00133
0.7306	606.90	-154.66	423.97	477.03	-0.00220	0.00095	0.00125
0.7393	606.67	-147.85	425.91	487.10	-0.00202	0.00085	0.00117
0.7480	606.45	-141.18	427.62	496.98	-0.00185	0.00076	0.00109
0.7567	606.24	-134.64	429.12	506.64	-0.00169	0.00068	0.00101
0.7654	606.04	-128.23	430.40	516.10	-0.00154	0.00060	0.00094
0.7741	605.85	-121.95	431.49	525.36	-0.00139	0.00053	0.00086
0.7828	605.67	-115.80	432.37	534.40	-0.00125	0.00046	0.00079
0.7915	605.49	-109.78	433.06	543.23	-0.00112	0.00040	0.00072
0.8001	605.33	-103.88	433.56	551.86	-0.00099	0.00035	0.00065
0.8088	605.17	-98.11	433.88	560.27	-0.00087	0.00029	0.00058
0.8175	605.01	-92.45	434.02	568.48	-0.00075	0.00025	0.00051
0.8262	604.87	-86.92	434.00	576.47	-0.00064	0.00020	0.00044
0.8349	604.73	-81.50	433.81	584.25	-0.00054	0.00016	0.00037
0.8436	604.59	-76.19	433.47	591.82	-0.00044	0.00013	0.00031
0.8523	604.47	-71.00	432.98	599.18	-0.00034	0.00010	0.00024
0.8610	604.34	-65.91	432.35	606.34	-0.00025	0.00007	0.00018
0.8697	604.23	-60.94	431.59	613.29	-0.00017	0.00004	0.00012

0.8784	604.12	-56.07	430.70	620.04	-0.00009	0.00002	0.00006
0.8870	604.01	-51.31	429.71	626.57	-0.00001	0.00000	0.00001
0.8957	599.07	-46.66	425.45	627.25	0.00000	0.00000	0.00000
0.9044	593.76	-42.15	420.94	627.25	0.00000	0.00000	0.00000
0.9131	588.66	-37.76	416.55	627.25	0.00000	0.00000	0.00000
0.9218	583.75	-33.50	412.29	627.25	0.00000	0.00000	0.00000
0.9305	579.03	-29.36	408.14	627.25	0.00000	0.00000	0.00000
0.9392	574.48	-25.33	404.11	627.25	0.00000	0.00000	0.00000
0.9479	570.11	-21.41	400.19	627.25	0.00000	0.00000	0.00000
0.9566	565.91	-17.60	396.38	627.25	0.00000	0.00000	0.00000
0.9652	561.86	-13.89	392.67	627.25	0.00000	0.00000	0.00000
0.9739	557.96	-10.27	389.06	627.25	0.00000	0.00000	0.00000
0.9826	554.21	-6.76	385.54	627.25	0.00000	0.00000	0.00000
0.9913	550.59	-3.33	382.12	627.25	0.00000	0.00000	0.00000
1.0000	547.11	0.00	378.78	627.25	0.00000	0.00000	0.00000

U.S. GOVERNMENT PRINTING OFFICE 750-112